

FUNDAMENTAL NEUTRON PHYSICS

Jeffrey S. Nico¹ and W. Michael Snow²

¹*National Institute of Standards and Technology, Gaithersburg, MD 20899-8461;
email: jnico@nist.gov*

²*Indiana University and Indiana University Cyclotron Facility, Bloomington, IN 47408;
email: snow@iucf.indiana.edu*

Key Words cold neutrons, CKM matrix, discrete symmetries, electroweak interactions, parity violation, ultracold neutrons

■ **Abstract** Experiments using slow neutrons address a growing range of scientific issues spanning nuclear physics, particle physics, astrophysics, and cosmology. The field of fundamental physics using neutrons has experienced a significant increase in activity over the last two decades. This review summarizes some of the recent developments in the field and outlines some of the prospects for future research.

CONTENTS

1. INTRODUCTION	28
1.1. Overview	28
1.2. Neutron Sources	30
2. NEUTRON DECAY AND STANDARD MODEL TESTS	33
2.1. Theoretical Framework	33
2.2. Neutron Lifetime Experiments	35
2.3. Angular Correlation Experiments	37
3. SEARCHES FOR NONSTANDARD <i>T</i> AND <i>B</i> VIOLATION	40
3.1. EDM Theoretical Framework	41
3.2. Electric Dipole Moment Experiments	43
3.3. <i>T</i> -Violation in Neutron Beta Decay	44
3.4. <i>D</i> - and <i>R</i> -Coefficient Measurements	45
3.5. <i>T</i> -Violation in Neutron Optics	46
3.6. Neutron-Antineutron Oscillations	47
4. NEUTRON-NUCLEON WEAK INTERACTIONS	47
4.1. Overview	48
4.2. Theoretical Description	50
4.3. Parity-Odd Neutron Spin Rotation and Capture Gamma Asymmetries	51
4.4. Test of Statistical Theories for Heavy Nuclei Matrix Elements	52
5. LOW ENERGY QCD TESTS	54
5.1. Theoretical Developments in Few Nucleon Systems and the Connection to QCD	54
5.2. Precision Scattering Length Measurements Using Interferometric Methods ..	55

5.3. Neutron-Electron Interaction	57
5.4. Neutron Polarizability	58
6. NEUTRONS IN ASTROPHYSICS AND GRAVITY	59
6.1. Big Bang Nucleosynthesis	59
6.2. Stellar Astrophysics	60
6.3. Gravitationally Induced Phase Shift	60
6.4. UCN Gravitational Bound States	61
7. SUMMARY	62

1. INTRODUCTION

1.1. Overview

The field of neutron physics has become an integral part of investigations into an array of important issues that span fields as diverse as nuclear and particle physics, fundamental symmetries, astrophysics and cosmology, fundamental constants, gravitation, and the interpretation of quantum mechanics. The experiments employ a diversity of measurement strategies and techniques, including condensed matter and low temperature physics, optics, and atomic physics, as well as nuclear and particle physics, and they address a wide range of issues. Nevertheless, the field possesses a coherence that derives from the unique properties of the neutron as an electrically neutral, strongly interacting, long-lived unstable particle that can be used either as the probe or as an object of study. This review covers some of the important new contributions that neutrons have made in these diverse areas of science. By “fundamental” neutron physics, we mean that class of experiments using slow neutrons which primarily address issues associated with the Standard Model (SM) of the strong, weak, electromagnetic, and gravitational interactions and their connection with issues in astrophysics and cosmology.

Neutrons experience all known forces in strengths that make them accessible to experimentation. It is an amusing fact that the magnitude of the average neutron interaction energy in matter, in laboratory magnetic fields, and near the surface of the Earth is the same order of magnitude for all forces except the weak interaction. This coincidence leads to unique and occasionally bizarre experimental strategies for measurements and a unique opportunity to search for gravitational effects on an elementary particle. The experiments include measurement of neutron-decay parameters, the use of parity violation to isolate the weak interaction between nucleons, and searches for a source of time reversal violation beyond the SM. These experiments provide information that is complementary to that available from existing accelerator-based nuclear physics facilities and high-energy accelerators. Neutron physics measurements also address questions in astrophysics and cosmology. The theory of Big Bang Nucleosynthesis needs the neutron lifetime and the vector and axial vector weak couplings as input, and neutron cross sections on unstable nuclei are necessary for a quantitative understanding of element creation in the universe.

TABLE 1 Common terminology and spectrum of neutron energies

Term	Energy	Velocity (m/s)	Wavelength (nm)	Temperature (K)
ultracold	$<0.2 \mu\text{eV}$	<6	>64	<0.002
very cold	$0.2 \mu\text{eV} \leq E < 50 \mu\text{eV}$	$6 \leq v < 100$	$4 < \lambda \leq 64$	$0.002 \leq T < 0.6$
cold	$0.05 \text{ meV} < E \leq 25 \text{ meV}$	$100 < v \leq 2200$	$0.18 \leq \lambda < 4$	$0.6 < T \leq 300$
thermal	25 meV	2200	0.18	300
epithermal	$25 \text{ meV} < E \leq 500 \text{ keV}$	$2200 < v \leq 1 \times 10^7$		
fast	$>500 \text{ keV}$	$>1 \times 10^7$		

Free neutrons are unstable with a 15 minute lifetime but are prevented from decaying while bound in nuclei through the combined effects of energy conservation and Fermi statistics. They must be liberated from nuclei using nuclear reactions with MeV-scale energies in order to be used and studied. We define “slow” neutrons to be neutrons whose energy has been lowered well below this scale. The available dynamic range of neutron energies for use in laboratory research is quite remarkable, as shown in Table 1. Thermodynamic language is used to describe different regimes; a neutron in thermal equilibrium at 300 K has a kinetic energy of only 25 meV. Because its de Broglie wavelength (0.18 nm) is comparable to interatomic distances, this energy also represents the boundary below which coherent interactions of neutrons with matter become important. The most intense sources of neutrons for experiments at thermal energies are nuclear reactors, although accelerators can also produce higher energy neutrons.

Neutron decay is an important process for the investigation of the Standard Model of electroweak interactions. As the prototypical beta decay, it is sensitive to certain SM extensions in the charged-current electroweak sector. Neutron decay can determine the Cabibbo-Kobayashi-Maskawa (CKM) matrix element $|V_{ud}|$ through increasingly precise measurements of the neutron lifetime and the decay correlation coefficients.

Searches for violations of time-reversal symmetry and/or CP symmetry address issues which lie at the heart of cosmology and particle physics. Among the important issues that can be addressed by neutron experiments is the question of what mechanisms might have led to the observed baryon asymmetry of the universe. Big Bang cosmology and the observed baryon asymmetry of the universe appear to require significantly more T -violation among quarks in the first generation than is predicted by the SM. The next generation of neutron electric dipole moment (EDM) searches, which plan to achieve sensitivities of $10^{-27} e \cdot \text{cm}$ to $10^{-28} e \cdot \text{cm}$, is the most important of a class of experiments aiming to search for new physics in the T -violating sector.

The last decade has also seen qualitative advances in both the quantitative understanding of nuclei, especially few-body systems, and in the connection between

nuclear physics and quantum chromodynamics (QCD). Low energy properties of nucleons and nuclei, such as weak interactions in n - A systems, low energy n - A scattering lengths, and the internal electromagnetic structure of the neutron (its electric polarizability and charge radius) are becoming calculable. These theoretical developments are motivating renewed experimental activity to measure undetermined low energy properties, such as the weak interaction amplitudes between nucleons, and to improve the precision of other low energy neutron measurements. The ultimate goal is to illuminate the strongly interacting ground state of QCD, the most poorly understood sector of the SM.

This review presents and discusses the status of the experimental efforts to confront these physics questions using slow neutrons. The improvements in precision required to address these questions are technically feasible and have spurred both new experimental efforts and the development of new neutron sources. We also discuss some of the new proposed facilities under construction. It is not possible to cover the large volume of work in a review of this scope, so we refer the reader to a number of more specialized reviews wherever appropriate. Instead, we emphasize recent experiments and those planned for the near future. Neutron experiments form part of a larger subclass of low energy precision measurements which test the SM (1). There are texts that cover a broader survey of topics and provide historical context (2–4). Tests of quantum mechanics using neutron interferometry are not discussed but are covered in detail in a recent comprehensive text (5).

1.2. Neutron Sources

Most fundamental neutron physics experiments are conducted with slow neutrons for two main reasons. First, slower neutrons spend more time in an apparatus. Second, slower neutrons can be more effectively manipulated through coherent interactions with matter and external fields. Free neutrons are usually created through either fission reactions in a nuclear reactor or through spallation in high Z targets struck by GeV proton beams. We briefly examine these neutron sources and the process by which cold and ultracold neutrons (UCN) are produced starting from neutrons with energies several orders of magnitude greater.

Neutrons are produced from fission in a research reactor at an average energy of approximately 2 MeV. They are slowed to thermal energy in a moderator such as heavy or light water, graphite, or beryllium, surrounding the fuel. The peak core fluence rate of research reactors is typically in the range $10^{14} \text{ cm}^{-2} \text{ s}^{-1}$ to $10^{15} \text{ cm}^{-2} \text{ s}^{-1}$. To maximize the neutron density, it is necessary to increase the fission rate per unit volume, but the power density is ultimately limited by heat transfer and material properties. In the spallation process, protons typically are accelerated to energies in the GeV range and strike a high Z target, producing approximately 20 neutrons with energies in the fast and epithermal region (6). This is an order of magnitude with more neutrons per nuclear reaction than from fission. Present spallation sources yield neutron rates of 10^{16} s^{-1} and 10^{17} s^{-1} . Although the time-averaged fluence from spallation neutron sources is about an order of

magnitude lower than for fission reactors, there is potentially more room for technical improvements in the near-term future.

The main feature that differentiates spallation sources from reactors is the possibility for operation in pulsed mode. At reactors one obtains continuous beams with a thermalized Maxwellian energy spectrum. In a spallation source, neutrons arrive at the experiment while the production source is off, and the frequency of the pulsed source can be chosen so that slow neutron energies can be determined by time-of-flight methods. The lower radiation background and convenient neutron energy information can be advantageous for certain experiments.

Fast neutrons reach the thermal regime most efficiently through a cascade of roughly 20 collisions with matter rich in hydrogen or deuterium. Cold neutrons are produced by a cryogenic neutron moderator adjacent to the reactor core or spallation target held at a temperature of ≈ 20 K. One generally wants the moderator as cold as possible to increase the phase space density of the neutrons. As the neutron wavelengths become large compared to the atomic spacings, the total scattering cross sections in matter are dominated by elastic or quasielastic processes, and it becomes more difficult for the neutrons to thermalize.

It is not practical to describe specific neutron facilities in any detail in this review, but we note a few where the bulk of research efforts have been carried out. For 30 years the most active facility for fundamental neutron research has been the Institut Max von Laue—Paul Langevin (ILL) in Grenoble, France (7). Its 58 MW reactor is the focal point of neutron beta-decay and UCN physics in the world. The new FRM-II reactor has come online in Munich with a predicted cold neutron fluence comparable to the ILL; its beamline for fundamental neutron physics is under construction (8). The most active institutions in the United States are the National Institute of Standards and Technology (NIST) (9) and Los Alamos National Laboratory (LANL) (10). In Russia, there are significant efforts at the Petersburg Nuclear Physics Institute (PNPI), Joint Institute for Nuclear Research (JINR) in Dubna, and the Kurchatov Institute and in Japan at the High Energy Accelerator Research organization (KEK). Many smaller sources play an essential role in the development of experimental ideas and techniques.

In addition to the existing sources, the last decade has seen tremendous growth in the construction of facilities and beamlines devoted to fundamental neutron physics. Many of these new facilities are at spallation sources. The Paul Scherrer Institut (PSI), which operates a continuous spallation source, has constructed a cold neutron beamline dedicated to fundamental physics (11). In the United States, the 2 MW Spallation Neutron Source (SNS) is under construction, and the fundamental physics beamline (FNPB) should be operational some time in 2008 (12). The Japanese Spallation Neutron Source (JSNS) is in the construction phase and is also anticipated to become operational in 2008. Tables 2 and 3 give a few of the measured (or projected) cold-neutron beam properties for some of the facilities with active fundamental physics programs.

In the neutron energy spectrum from a cold moderator, there is a very small fraction whose energies lie below the ≈ 100 neV neutron optical potential of matter.

TABLE 2 Some operating parameters for major cold neutron reactor-based user facilities with active (and proposed) fundamental physics programs. Fluence rates are given as neutron capture fluence

Parameter	ILL PF1	ILL PF2	NIST NG-6	(FRM-II) (Mephisto)
Power (MW)	58	58	20	(20)
Guide length (m)	60	74	68	(30)
Guide radius (m)	4000	4000	∞	(460)
Guide type ($m=$)	1.2	2	1.2	(3)
Cross section (cm ²)	6×12	6×20	6×15	(5×11.6)
Fluence rate ($\times 10^9$ cm ⁻² s ⁻¹)	4	14	2	(20)

Such neutrons are called ultracold neutrons, and they can be trapped by total external reflection from material media. The existence of such neutrons was established experimentally in the late 1960s (13, 14). The UCN facility at the ILL employs a turbine to mechanically convert higher energy neutrons to UCN (15). Although the density of neutrons is bounded by the original phase space in the source (Liouville's theorem), this technique produces enough UCN to conduct a number of unique and fundamental experiments described in part below. During the last decade new types of UCN converters have been developed that can increase the phase space density through the use of "superthermal" techniques (16). They involve energy dissipation in the moderating medium (through phonon or magnon creation) and therefore are not limited by Liouville's theorem. Superfluid helium (17) and solid deuterium (18) have been used successfully as superthermal UCN sources, and solid oxygen is also being studied (19). The lack of neutron absorption in ⁴He along with its other unique properties makes possible experiments in

TABLE 3 Some operating parameters for major cold neutron spallation-source user facilities with active (and proposed) fundamental physics programs. Fluence rates are given as neutron capture fluence

Parameter	SINQ FunSpin	LANSCE FP12	(SNS) (FNPB)	(JSNS)
Time-averaged current (mA)	1.2	0.1	(1.4)	(0.3)
Source rep. rate (Hz)	dc	20	(60)	(25)
Guide length (m)	7	8	(15)	(10 to 20)
Guide radius (m)	∞	∞	(117)	(∞)
Guide type ($m=$)	3	3	(3.5)	(3)
Cross section (cm ²)	4×15	9.5×9.5	(10×12)	(10×10)
Fluence rate ($\times 10^8$ cm ⁻² s ⁻¹)	8	1	(10)	(5)

which the measurement is conducted within the moderating medium. These developments have led to proposals for new UCN facilities at LANL, PSI, FRM-II (Forschungsreaktor München II), KEK, North Carolina State, Mainz, and other sources. Extensive treatments of UCN physics are found in References (20, 21).

2. NEUTRON DECAY AND STANDARD MODEL TESTS

Several reviews discuss weak interaction physics using slow neutrons in greater detail or provide additional information (22–24). A recent publication addresses the issue of CKM unitarity (25). A comprehensive review of measurements in neutron and nuclear beta decay to test the SM in the semileptonic sector and its possible extensions along with a comparison with other probes of similar physics will appear in the near future (26).

2.1. Theoretical Framework

The neutron is composed of two down quarks and an up quark, and it is stable under the strong and electromagnetic interactions, which conserve quark flavor. The weak interaction can convert a down quark into an up quark through the emission of the W gauge boson. The mass difference of the neutron and proton is so small that the only possible decay products of the W are an electron and antineutrino with the release of energy distributed among all the decay products: $n \rightarrow p + e^- + \bar{\nu}_e + 0.783 \text{ MeV}$. Neither of the other available decay modes, radiative neutron decay with a photon in the final state or decay to a hydrogen atom and an antineutrino, have been seen yet, although the first searches for radiative decay are in progress (28, 29). Experiments test the assumptions of the SM by performing precision measurements on the proton and electron energies and momenta and the neutron spin.

To leading order, free neutron decay in the SM is described by a mixed vector/axial-vector current characterized by two coupling strengths, g_V and g_A , the vector and axial-vector coupling coefficients. Because the momentum transfers involved in neutron beta decay are small compared to the W and Z masses, one can write an effective Lagrangian that describes neutron decay in the SM as a four-fermion interaction

$$\mathcal{L}_{int} = \frac{G_F V_{ud}}{2\sqrt{2}} (V_\mu - \lambda A_\mu)(v^\mu - a^\mu), \quad 1.$$

where $V_\mu = \bar{\psi}_p \gamma_\mu \psi_n$, $v^\mu = \bar{\psi}_e \gamma^\mu \psi_\nu$, $A_\mu = \bar{\psi}_p \gamma_\mu \gamma_5 \psi_n$, and $a^\mu = \bar{\psi}_e \gamma^\mu \gamma_5 \psi_\nu$ are the hadronic and leptonic vector and axial vector currents constructed from the neutron, proton, electron, and neutrino fermion fields, G_F is the Fermi decay constant, V_{ud} is a CKM matrix element, and λ is the ratio of the axial vector and vector couplings.

The V-A structure for the weak currents is incorporated directly into the standard electroweak theory by restricting the weak interaction to operate only on

the left-handed components of the quark and lepton fields. A more fundamental understanding of the reason for this parity-odd structure of the weak interaction is still lacking. There is also no understanding for the values of the CKM mixing matrix elements between the quark mass eigenstates and their weak interaction eigenstates. The fact that the matrix is unitary is ultimately a consequence of the universality of the weak interaction gauge theory. Extensions to the SM which either introduce non V-A weak currents or generate violations of universality can therefore be tested through precision measurements in beta decay. A recent reanalysis of the constraints on non V-A charged currents showed that improved neutron decay measurements have set new direct limits on such couplings, which are typically constrained at the 5% level (26). Complementary constraints on non V-A charged currents in neutron beta decay from neutrino mass limits have recently appeared (27).

The probability distribution for beta decay in terms of the neutron spin and the energies and momenta of the decay products (30) can be written

$$dW \propto (g_V^2 + 3g_A^2)F(E_e) \left[1 + a \frac{\vec{p}_e \cdot \vec{p}_\nu}{E_e E_\nu} + b \frac{m_e}{E_e} + \vec{\sigma}_n \cdot \left(A \frac{\vec{p}_e}{E_e} + B \frac{\vec{p}_\nu}{E_\nu} + D \frac{\vec{p}_e \times \vec{p}_\nu}{E_e E_\nu} \right) \right], \quad 2.$$

where one defines

$\tau_n = \frac{2\pi^3 \hbar^7}{m_e^5 c^4} \frac{1}{f(1 + \delta_R)(g_V^2 + 3g_A^2)}$	$= (885.7 \pm 0.8) \text{ s}$	neutron lifetime
$\lambda = \left \frac{g_A}{g_V} \right e^{i\phi}$	$= -1.2695 \pm 0.0029$	coupling constant ratio
$a = \frac{1 - \lambda ^2}{1 + 3 \lambda ^2}$	$= -0.103 \pm 0.004$	electron-antineutrino asymmetry
$b = 0$	$= 0$	Fierz interference
$A = -2 \frac{ \lambda ^2 + \lambda \cos \phi}{1 + 3 \lambda ^2}$	$= -0.1173 \pm 0.0013$	spin-electron asymmetry
$B = 2 \frac{ \lambda ^2 - \lambda \cos \phi}{1 + 3 \lambda ^2}$	$= 0.983 \pm 0.004$	spin-antineutrino asymmetry
$D = 2 \frac{ \lambda \sin \phi}{1 + 3 \lambda ^2}$	$= (-0.6 \pm 1.0) \times 10^{-3}$	T-odd triple-product.

In these equations, which neglect small corrections such as weak magnetism, $F(E_e)$ is the electron energy spectrum, \vec{p}_e , \vec{p}_ν , E_e , and E_ν are the momenta and kinetic energies of the decay electron and antineutrino, $\vec{\sigma}_n$ is the initial spin of the decaying neutron, ϕ is the phase angle between the weak coupling constants g_A and g_V , and $f(1 + \delta_R) = 1.71489 \pm 0.00002$ is a theoretically calculated phase space factor (31). The spin-proton asymmetry correlation coefficient C is proportional to the quantity $A + B$. The values represent the world averages as compiled by the Particle Data Group (PDG) (32). The parameter λ can be extracted from measurement of either a , A , or B . If the neutron lifetime τ_n is also measured, g_V and g_A can be determined uniquely under the assumption that $D = 0$. Figure 1 shows the recent history of measured values of the lifetime and correlation coefficients as used by the PDG (32).

One strong motivation for more accurate measurements of neutron decay parameters is to measure $|V_{ud}|$. The most precise number comes from the $\mathcal{F}t$ values of superallowed $0^+ \rightarrow 0^+$ β transitions between isobaric analog states (33). This gives $|V_{ud}| = 0.0738 \pm 0.0004$ with the uncertainty dominated by theoretical corrections. Using values of $|V_{us}|$ and $|V_{ub}|$ taken from the current recommendations of the PDG, $|V_{ud}|^2 + |V_{us}|^2 + |V_{ub}|^2 = 0.9966 \pm 0.0014$ value differs from unitarity by 2.1 standard deviations.

Neutron beta decay offers a theoretically cleaner environment for extracting g_V due to the absence of other nucleons (although some radiative corrections are common to both systems). Using the PDG values of τ_n and λ , the same unitarity test gives $\sum_i |V_{ui}|^2 = 0.9971 \pm 0.0039$, consistent with unity but less precise. This result agrees with both the nuclear result and unitarity. The present situation regarding unitarity is summarized in Figure 2. Pion beta decay is theoretically the cleanest system in which to measure $|V_{ud}|$, but the small branching ratio has so far precluded a measurement with enough sensitivity to compete with superallowed beta decay and neutron decay. The latest measurement from pion beta decay gives $|V_{ud}| = 0.9728 \pm 0.0030$ (34).

The possible deviation from unitarity has motivated a number of new precise measurements of semileptonic kaon decay rates which promise to determine $|V_{us}|$ more precisely (35). If one were use the value of $|V_{us}|$ from some recent evaluations (36), the discrepancy with unitarity disappears. There are also renewed theoretical investigations to extract $|V_{us}|$ from hyperon decay (37). A precision determination of $|V_{ud}|$ should be seen in the context of the overall effort to determine with high precision all the parameters of the CKM matrix. The CLEO-c collaboration of the Cornell Electron Storage Ring should measure the CKM matrix element $|V_{cd}|$ to 1% accuracy if lattice gauge theory calculations of the required form factors can match the expected precision of the data (36, 38). This would make possible another independent check of CKM unitarity using the first column, $|V_{ud}|^2 + |V_{cd}|^2 + |V_{td}|^2 = 1$.

2.2. Neutron Lifetime Experiments

Seven experiments (39–45) contribute to a neutron lifetime world average of $\tau_n = (885.7 \pm 0.8)$ s (32). The experiments employ one of two distinct experimental strategies for measuring the neutron lifetime. The four more precise measurements use ultracold neutrons that are confined using a combination of material walls and gravity. One fills the trap and measures the number of neutrons remaining as a function of time to extract τ . An advantage of this technique is that one avoids the necessity of knowing the absolute neutron density and detector efficiency. The measured value of τ is $(1/\tau_n + 1/\tau_{loss})^{-1}$ and includes losses from the trap as well as neutron decay. To isolate τ_{loss} , which is typically dominated by nonspecular processes in the neutron interaction with the trap walls, one measures τ in bottles with different surface-to-volume ratios and performs an extrapolation to an infinite volume. These losses depend on the UCN energy spectrum, which

can change during the storage interval, so much work has been done to understand the spectrum evolution and loss mechanisms and to find surface materials with lower loss probabilities.

To address losses experimentally, Arzumanov et al. simultaneously measured the UCN storage time and the inelastically scattered neutrons (44), thus monitoring the primary loss process. An experiment by Serebrov et al. (46) achieved a significant reduction in wall losses by using low temperature fomblin oil. This coating produced very long storage times and permitted much shorter extrapolations in collision frequency. The result is very different (6.5σ) from the PDG average, as illustrated in Figure 1. The group intends to make additional measurements with a variable-volume trap to change the collision frequency while maintaining the same trap surface and vacuum conditions.

The second method measured simultaneously both the rate of neutron decays dN/dt and the average number of neutrons N in a well-defined volume of a neutron beam. The neutron lifetime was determined from the differential form of the radioactive decay function, $dN/dt = -N/\tau_n$. Such a measurement requires accurate absolute counting of neutrons and neutron decay products (protons) from a cold neutron beam and must overcome its own set of technical challenges. The two more precise experiments used a segmented proton trap (47) and a neutron detector with an efficiency that was proportional to $1/v$ (48, 49). Both experiments produced a value in good agreement with the PDG average.

Accurate measurements using each of these completely independent methods are important for establishing the reliability of the results for τ_n . The latest measurement is in dramatic disagreement with existing values, and the situation must be resolved by new experiments.

2.2.1. FUTURE PROSPECTS IN NEUTRON LIFETIME MEASUREMENTS A third approach to measuring τ_n avoids many of these problems. The most natural way to measure exponential decay is to acquire an ensemble of radioactive species and register the decay products. One can then simply fit the time spectrum for the slope, or decay rate, of the exponential function. Such a measurement using neutrons has only become feasible after the demonstration of magnetically trapping UCNs in superfluid ^4He (50). The UCNs fill a magnetic trap through the inelastic scattering of 0.89 nm neutrons in superfluid ^4He (the superthermal process). As the trapped neutrons beta decay, the energetic electrons are registered via scintillations in the helium, thus allowing one to fit directly for the exponential decay.

The experiment initially observed a short lifetime and attributed it to the presence of neutrons with energies higher than the magnetic potential of the trap. When the magnetic field was ramped to eliminate these neutrons, the result is in agreement with the currently accepted value of the free neutron lifetime, but the statistical uncertainty is large (60 s) (51). Upgrades to the apparatus are in progress to increase the number of trapped neutrons. The collaboration anticipates that a statistical precision of a few seconds will be possible in the near future.

There are two new bottle-type UCN experiments in the developmental stage. The first uses a low temperature fomblin oil to reduce the collisional losses.

Recent data demonstrate a UCN reflection loss coefficient of 5×10^{-6} when the vessel temperature is in the range of 105 K to 150 K. They intend to use this surface coating in an “accordion-like” storage vessel, thus allowing one to vary the trap volume while keeping the surface area and characteristics constant (52). The collaboration expects to achieve a precision of 1 s. The second experiment will store UCN magnetically in vacuum using an arrangement of permanent magnets and superconducting solenoids and extract the protons electrostatically. The lifetime is measured by real-time detection of the decay protons and counting the integral number of neutrons using different storage times (53). The collaboration anticipates that a measurement with 0.1 s uncertainty is possible.

2.3. Angular Correlation Experiments

2.3.1. SPIN-ELECTRON ASYMMETRY A With the neutron lifetime and one of the correlation coefficients a , A , or B , one can determine values for g_A and g_V . Because it has the greatest sensitivity to λ and is more accessible experimentally, the spin-electron asymmetry A has been measured more frequently and with greater precision. Four independent measurements used in the PDG evaluation are not in good agreement with each other, so the PDG uses a weighted average for the central value and increases the overall uncertainty by a scale factor of 2.3 (32). We discuss the two more recent measurements, one using a time projection chamber and one using an electron spectrometer, and the prospects for future improvement.

In the experiment of Schreckenbach et al. (54), a beam of polarized cold neutrons was surrounded by a time projection chamber (TPC). Decay electrons passed through the drift chamber and were incident on plastic scintillators. The drift chamber recorded the ionization tracks in three dimensions while the scintillator gave the electron energy and start signal for the drift chamber. The TPC provided good event identification and reduced gamma ray backgrounds. The result was $A = -0.1160 \pm 0.0015$ (55). The contributions to the overall uncertainty were roughly split between statistical and systematic uncertainties with the largest systematic contribution coming from the background subtraction.

The PERKEO II experiment also used a beam of cold polarized neutrons, but the decay electrons were extracted using a superconducting magnet in a split pair configuration. The field was transverse to the beam, so neutrons passed through the spectrometer but electrons were guided by the field to one of two scintillator detectors on each end. This arrangement had the advantage of achieving a 4π acceptance of electrons. An asymmetry is formed from the electron spectra in the two detectors as a function of the electron energy; the difference in those quantities for the two detectors is directly related to the electron asymmetry. Their run produced $A = -0.1178 \pm 0.0007$, where the main contributions to the uncertainty were in the neutron polarimetry, background subtraction, and electron detector response (56).

The next version of PERKEO II will use the new ballistic supermirror guide at the ILL with four times the fluence rate (57). The collaboration intends to use a new configuration of crossed supermirror polarizers to make the neutron polarization more uniform in phase space (58). The beam polarization can also be measured

with a completely different method using an opaque ^3He spin filter. PERKEO II anticipates reducing the main correction and uncertainty in the polarization analysis from 1.1% to less than 0.25% with an uncertainty of 0.1% in that value.

There are several other efforts underway to perform independent measurements of the electron asymmetry. The UCNA collaboration has made progress toward measuring A using a superconducting solenoidal spectrometer (59). UCNs are produced in a solid deuterium moderator at the Los Alamos Neutron Science Center (LANSCE) and transported to the spectrometer using diamond-coated guides. In the spectrometer, one produces highly polarized ($>99.9\%$) neutrons by passing them through a 6 T magnetic field and into an open ended cylinder which increases the dwell time of the polarized UCN in the decay spectrometer. The decay electrons will be transported along the field lines to detectors at each end of the spectrometer. The detectors consist of multiwire proportional counters backed by plastic scintillator. The collaboration believes that a 0.2% measurement is possible with three weeks of running.

Two other groups propose measuring the A coefficient at the 10^{-3} level. The detector designs allow the possibility of measuring other decay correlation coefficients with the same apparatus. A group at PNPI is working on a magnetic spectrometer to be used with a highly collimated cold neutron beam. The field guides decay particles to an electron detector at one end and a proton detector at the other. Their neutron polarimeter agrees with ^3He -based spin filter methods at the $\approx 2 \times 10^{-3}$ level (60). The spectrometer should also be able to measure the coefficients A and B simultaneously, thus eliminating the need for precision polarimetry.

The abBA collaboration proposes to use an electromagnetic spectrometer that guides both decay electrons and protons to detectors at each end of the spectrometer (61). The detector would be able to measure a , A , B , and the Fierz interference term b , which is zero in the SM. The detectors would be large-area segmented silicon detectors with thin entrance windows that allow the detection of both the proton and electron. The ability to detect coincidences greatly suppresses backgrounds and allows the measurement of residual backgrounds. The magnetic field guides the decay products to conjugate points on the segmented Si detectors and provides 4π detection of both electrons and protons and suppression of backgrounds by use of coincidences. The apparatus is being designed for use at a pulsed spallation source to exploit background reduction and perform neutron polarimetry. The neutrons can be polarized by transmission through polarized ^3He , whose spin-dependent absorption cross section possesses an accurately known neutron energy dependence that can be exploited for accurate neutron polarization measurement (62).

2.3.2. SPIN-ANTINEUTRINO ASYMMETRY B The electron asymmetry and antineutrino asymmetry provide complementary information. g_A is equal to -1 in the SM Lagrangian at the quark level but is renormalized in hadrons by the strong interaction. Because g_A is nearly -1 , A is close to zero, and B is near unity. Thus B

is not particularly sensitive to λ but provides more attractive ground for searching for non-SM signatures, such as extended left-right symmetric models.

Left-right symmetric models, which are motivated in part by the desire to restore parity conservation at high energy scales, add a new right-handed charged gauge-boson W_2 with mass M_2 and four new parameters to be constrained by experiments: a mixing angle ζ , $\delta = (M_1/M_2)^2$, $r_g = g_R/g_L$ the ratio of the right- and left-handed gauge coupling strengths g_R and g_L , and $R_K = V_{ud}^R/V_{ud}^L$ where R and L designate the right and left sectors. In the manifest left-right symmetric model (MLRM), $r_g = r_K = 1$, and in the SM $\delta = 0$.

The mass limit on a right-handed vector boson comes from muon decay and is 406 GeV/ c^2 (63). In the MLRM where there are only two parameters (ζ and δ), constraints from other systems are better than the neutron constraints. For the extended left-right model, however, neutron-derived constraints are complementary to the other searches. Another area in which to search for right-handed currents is the decay of the neutron into a hydrogen atom and antineutrino, because one of the hyperfine levels of hydrogen cannot be populated unless right-handed currents are present (64). The small branching ratio has precluded a search so far.

In the last three decades, there have been only two new measurements of the antineutrino asymmetry. Because the antineutrino cannot be conveniently detected, its momentum was deduced from electron-proton coincidence measurements. Electrons from the decay of polarized neutrons were detected by plastic scintillators, and protons were detected by an assembly of two microchannel plates. From the electron energy and proton time-of-flight, one can reconstruct the antineutrino momentum. The first measurement was carried out at PNPI and produced a result of $B = 0.9894 \pm 0.0083$ (65). A second run at the ILL used largely the same apparatus and measured $B = 0.9821 \pm 0.0040$ (66), where the largest reduction in the overall uncertainty came from improved statistics.

A recent measurement of B was performed using the PERKEO II apparatus. Typically, one detects electron-proton coincidences using one detector for each particle. The PERKEO II measurement uses two detectors, one in each hemisphere of the detector, that can detect both electrons and protons. Electrons are detected using plastic scintillator, while the protons are accelerated on a thin carbon foil placed in front of the scintillator. The resulting secondary electrons are guided onto the electron detectors. This technique reduces systematics and increases the sensitivity to B .

2.3.3. ELECTRON-ANTINEUTRINO ASYMMETRY a Although the electron-antineutrino asymmetry a has approximately the same sensitivity to λ as A , it is only known to 4%. Since 1978 (67), there has been only one new measurement. The experimental difficulty lies with the energy measurement of the recoil protons, whose spectral shape is slightly distorted for nonzero a . Unlike A , it does not require neutron polarimetry. A precision measurement of a would produce an independent measurement of λ , an improved test of CKM unitarity, and model-independent tests of new physics. The values of a , A , and B can be related to the strength of

hypothetical right-handed weak forces and scalar and tensor forces (68, 69), and it was recently shown that a precise comparison of a and A can place stringent limits on possible conserved-vector-current (CVC) violation and second class currents in neutron decay (70).

The most recent determination of a comes from measurements of the integrated energy spectrum of recoil protons stored in an ion trap (71). A collimated beam of cold neutrons passed through a proton trap consisting of annular electrodes coaxial with a magnetic field whose strength varied from 0.6 T to 4.3 T over the length of the trap. Protons created inside the volume were trapped, and those created in a high field region were adiabatically focused onto a mirror in the low field region. The trap was periodically emptied and the protons counted as a function of the mirror potential. The result of $a = -0.1054 \pm 0.0055$ is in good agreement with the previous measurement and of comparable precision.

The precision of a measurements must be improved to the level of A experiments to constrain λ . There are two major efforts underway to improve the precision of a , a SPECT (72) and a CORN (73). a CORN relies on the measurement of an asymmetry in the coincidence detection of electrons and recoil proton that is proportional to a (74). The asymmetry is formed by carefully restricting the phase space for the decay in a magnetic spectrometer so that decay events with parallel and antiparallel electron and antineutrino momenta are separated in the coincidence timing spectrum. a is directly proportional to the relative number of events, and there is no need for precise spectroscopy of the low energy protons. The experiment will be built and tested at the Low Energy Neutron Source (LENS) (75) and then run at NIST where a measurement of approximately 1% accuracy is feasible.

In the a SPECT experiment, one again measures a proton energy spectrum as a function of a potential, similar to the idea used for the proton trap experiment. One increases the statistical power by completely separating the source part and the spectroscopy part of the apparatus. A cold neutron beam will pass through a region of strong, homogeneous magnetic field transverse to the beam. The decay protons with initial momentum component along the field direction will be directed toward a detector. Near the detector is a region of weaker magnetic field and electrostatic retardation potentials, and only those protons with sufficient energy to overcome the barrier continue on to the detector. Registering the protons as a function of the retardation potential gives the recoil proton spectrum, which one fits to extract a . The collaboration believes that a statistical uncertainty of approximately 0.25% is achievable.

3. SEARCHES FOR NONSTANDARD T AND B VIOLATION

The physical origins of the observed CP violation in nature, first seen in the neutral kaon system (76), remain obscure. CP violation implies T violation (and vice versa) through the CPT theorem. Recent experiments have reported measuring

CP violation in the $K_L^0 \rightarrow 2\pi$ amplitudes (77, 78) and in the decays of the neutral B -mesons (79, 80). The SM can accommodate the possibility of CP violation through a complex phase δ_{KM} in the CKM quark mixing matrix. To date there is no firm evidence against the possibility that the observed CP -violation effects are due to this phase (81), but the question remains whether or not there exist sources of CP -violation other than δ_{KM} . There is indirect evidence for this possibility from cosmology; it appears that δ_{KM} is not sufficient to generate the baryon asymmetry of the universe in the Big Bang model. One area to probe for the existence of new CP -violating interactions is systems involving first-generation quarks and leptons for which the contribution from δ_{KM} is typically suppressed. Examples of observables of this kind are electric dipole moments of the neutron, leptons, as well as atoms and T -odd correlations in leptonic and semileptonic decays.

3.1. EDM Theoretical Framework

The search for the neutron electric dipole moment addresses issues which lie at the heart of modern cosmology and particle physics. The current limit on the permanent EDM of the neutron represents one of the most sensitive null measurements in all of physics and has eliminated many theories and extensions to the SM (Figure 3). The reader is directed to a comprehensive review of EDM experiments by Ramsey (82) and more recently in References (24, 83).

The energy of a neutral spin-1/2 particle with an EDM d_n in an electric field \vec{E} is $E_n = -d_n \vec{\sigma} \cdot \vec{E}$, where $\vec{\sigma}$ is the Pauli spin matrix. This expression is odd under T and P . The current experimental bound on the neutron EDM is $d_n < 0.63 \times 10^{-25} e \cdot \text{cm}$ (90% CL) (32, 84). In the SM, there are two sources of CP violation. One source is the complex phase δ_{KM} in the CKM matrix. The other source is a possible term in the QCD Lagrangian itself, the so-called θ -term

$$\mathcal{L}_{QCD} = \mathcal{L}_{QCD, \theta=0} + \frac{\theta g_s^2}{32\pi^2} G_{\mu\nu} \tilde{G}^{\mu\nu}, \tag{3}$$

which explicitly violates CP symmetry because of the appearance of the product of the gluonic field operator G and its dual \tilde{G} . Because G couples to quarks but does not induce flavor change, d_n is much more sensitive to θ than it is to δ_{KM} . Thus, measurement of d_n determines an important parameter of the SM. Calculations have shown that $d_n \sim O(10^{-16}\theta) e \cdot \text{cm}$ (85, 86).

Although θ is unknown, the observed limit on d_n allows one to conclude that $\theta < 10^{-(9\pm 1)}$ (87). Because the natural scale is $\theta \sim O(1)$, the very small value for θ (known as the strong CP problem) requires an explanation. One attempt augments the SM by a global $U(1)$ symmetry (referred to as the Peccei-Quinn symmetry), whose spontaneous breakdown gives rise to Goldstone bosons called axions (88). The θ -term is then essentially eliminated by the vacuum expectation value of the axion. No axions have yet been observed.

Since CP violation through the phase in the CKM matrix involves flavor mixing of higher generation quarks, d_n is very small in the SM; calculations predict it to

be $10^{-32} e \cdot \text{cm}$ to $10^{-31} e \cdot \text{cm}$ (89, 90), several orders of magnitude beyond the reach of any experiment being considered at present. Models of new physics, including left-right symmetric models, non-minimal models in the Higgs sector, and supersymmetric (SUSY) models, allow for CP violating mechanisms not found in the SM, including terms that do not change flavor. Searches for electric dipole moments in the neutron, leptons, and atoms, which are particularly insensitive to flavor-changing parameters, can strongly constrain such models.

3.1.1. BARYON ASYMMETRY Antimatter appears to be rare in the universe, and there exists a substantial asymmetry between the number of baryons and antibaryons. Although the SM possesses a nonperturbative mechanism to violate the baryon number B , no experiments have seen B violation, and it is natural to speculate on the origin of the baryon asymmetry of the universe. There are two outstanding facts: baryons make up only 5% of the total energy density of the universe and the ratio of baryons to photons is very small. The ratio $n_B/n_\gamma = (6.1 \pm 0.3) \times 10^{-10}$ is known independently both from Big Bang Nucleosynthesis and fluctuations in the microwave background (91). Sakharov first raised the possibility of calculating the baryon asymmetry from basic principles (92). He identified three criteria that, if satisfied simultaneously, will lead to a baryon asymmetry from an initial $B = 0$ state: baryon number violation, CP violation, and departure from thermal equilibrium. One way to explain the asymmetry assumes that all three of these conditions were met at some very early time in the universe and that this physics will remain inaccessible to us, with the B asymmetry effectively an initial condition. However, the existence of inflation in the early universe—a scenario that generates a flat universe, solves various cosmological problems, and generates a spectrum of primordial density fluctuations consistent with observation—would dilute any such early B asymmetry to a negligible level. In this case the B asymmetry must be regenerated through later processes, and there is hope that it is calculable from first principles (93).

Although the SM contains processes that satisfy the first two conditions and the Big Bang satisfies the third, it fails by many orders of magnitude in its estimate of the size of the baryon asymmetry. Grand unified theory (GUT) baryogenesis at $T \sim 10^{29}$ K corresponding to a mass scale on the order of 10^{16} GeV is disfavored by inflation. Electroweak baryogenesis (95, 96), which relies on a nonperturbative $B - L$ -violating mechanism (where L is lepton number) present in the SM due to nonperturbative electroweak fields (97) combined with CP violation and a departure from equilibrium at the electroweak phase transition, is now very close to being ruled out (98). Leptogenesis (99, 100) combined with $B - L$ conserving processes to get the B asymmetry and the Affleck-Dine mechanism are the most favored speculations at the moment (101).

It appears that some physics beyond the SM, including new sources of CP violation that may lead to a measurable value for d_n , must exist if the observed baryon asymmetry is to be understood. The minimal supersymmetric extension of the SM (MSSM) (102) can possess small values of the CP -violating phases

(consistent with constraints from d_n) that generate the baryon asymmetry. Within the broad framework of non-minimal SUSY models, including GUTs, there are numerous new sources of CP violation in complex Yukawa couplings and other Higgs parameters that may have observable effects on the neutron EDM (103–105). The present limit on the neutron EDM already severely constrains many SUSY models.

3.2. Electric Dipole Moment Experiments

EDM experiments employ polarized neutrons with the Ramsey interferometric technique of separated oscillatory fields. Static electric E_0 and magnetic B_0 fields are applied to the polarized neutrons. The neutron spin state is then governed by the Hamiltonian $H = -\vec{\mu} \cdot \vec{B}_0 \pm \vec{d}_n \cdot \vec{E}_0$. A radio frequency (RF) magnetic field of frequency ω_a is applied to tilt the neutron polarization normal to E_0 and B_0 and it starts to precess with a frequency ω_R . After a free precession time T a second tilt pulse in phase with the first is applied and the neutron polarization direction is proportional to $(\omega_R - \omega_a)T$. The Larmor precession frequency of the neutron depends on the direction of the applied field E_0 relative to $\vec{\mu}$. An EDM would appear as a change in ω_R as the electric field is reversed.

The two most stringent limits on d_n come from Altarev et al. at PNPI (106) and Harris et al. at ILL (84). Both experiments used stored UCN. The PNPI apparatus contained two UCN storage chambers with oppositely directed electric fields. A nonzero EDM would cause frequency shifts of opposite sign in each of the chambers, and some sources of magnetic field noise are suppressed with simultaneous measurements with both fields. Nevertheless, slowly varying magnetic fields remained a significant source of systematic uncertainty. In the experiment of Harris et al., a polarized ^{199}Hg comagnetometer occupying approximately the same volume as the neutrons was introduced into the storage volume to continuously monitor the magnetic field. The comagnetometer was essential in eliminating stray magnetic fields as a major source of systematic uncertainty. The experimental accuracy was limited by neutron counting statistics.

There are ambitious efforts underway to improve the current neutron EDM limit by one to two orders of magnitude. All of the experiments attempt to increase the number of UCN, the observation time, and the size of the applied electric field. The CryoEDM collaboration intends to produce UCNs through the superthermal process and transport them to a separate measurement chamber containing superfluid helium. Liquid helium should allow electric field values that are several times larger than used in past experiments, and the cryogenically pure environment should permit longer UCN storage times. The collaboration proposes to use a multichamber spectrometer for compensation of field fluctuations by means of SQUID (superconducting quantum interference device) magnetometers.

The nEDM collaboration proposes to search for the neutron EDM with a double chamber storage cell to suppress magnetic field fluctuations, thus allowing one to extract d_n from the simultaneous measurement in chambers with opposite electric

field values. The magnetic field would be inferred from a set of laser optically pumped Cs magnetometers placed outside the storage cells. The UCN would be produced in the solid deuterium UCN source under construction at PSI.

A LANSCE-based EDM experiment under development (83) also proposes to increase the UCN density using downscattering of UCN in superfluid ^4He and exploit the large electric fields achievable in helium. The experiment will use polarized ^3He atoms as the comagnetometer in a bath of superfluid helium at a temperature of approximately 300 mK. The strong spin dependence of the ^3He neutron absorption cross section allows the relative orientation of the neutron and ^3He spins to be continuously monitored through the intensity of the scintillation light in the helium. One obtains d_n by measuring the difference in the neutron and ^3He precession frequencies for the different orientation of electric field.

There are also preparations underway to search for the neutron EDM using dynamical diffraction from noncentrosymmetric perfect crystals. In dynamical diffraction the incident neutron plane wave state $|k\rangle$ is split as it enters the crystal into two coherent branches $|k_+\rangle$ and $|k_-\rangle$ with slightly different momenta and energies. The probability density of these two states is concentrated along and in between the lattice planes, respectively. In noncentrosymmetric crystals the position of the electric field maxima can be displaced with respect to the nuclei. Therefore, one of the branches can experience interplanar electric field (10^9 V/cm), which are orders of magnitude larger than can be achieved through application of external fields (107, 108). The presence of a neutron EDM would produce an extra relative phase shift between the two interfering branches. Such experiments must contend with potentially large systematic effects such as those from neutron spin-orbit scattering from the atoms (109). A number of experiments which investigate neutron optical issues relevant for an eventual EDM measurement of this type have been performed recently.

3.3. *T*-Violation in Neutron Beta Decay

With its small SM values of time-reversal violating observables, neutron beta decay also provides an excellent laboratory in which to search for *T* violation. Leptoquark, left-right symmetric models, and exotic fermion models can all lead to violations of time-reversal symmetry at potentially measurable levels (110). One possible *T*-odd correlation in polarized neutron decay is $D\vec{\sigma}_n \cdot (\vec{p}_e \times \vec{p}_p)$, where \vec{p}_p is the momentum of the recoil proton. The *D* coefficient is sensitive only to *T*-odd interactions with vector and axial vector currents. In a theory with such currents, the coefficients of the correlations depend on the magnitude and phase of $\lambda = |\lambda|e^{-i\phi}$.

D has *T*-even contributions from phase shifts caused by pure Coulomb and weak magnetism scattering. The Coulomb term vanishes in lowest order in V-A theory (30), but scalar and tensor interactions could contribute. Fierz interference coefficient measurements (111, 112) can be used to limit this possible contribution to $|D^{EM}| < (2.8 \times 10^{-5}) \frac{m_e}{p_e}$. Interference between Coulomb scattering amplitudes

and the weak magnetism amplitudes produce a final state effect of order $E_e^2/p_e m_n$. This weak magnetism effect is predicted to be $|D^{WM}| = 1.1 \times 10^{-5}$ (113). Reference (110) summarizes the current constraints on D from analyses of data on other T -odd observables for the SM and extensions.

The EDM violates both T and P symmetries, whereas a D coefficient violates T but conserves P . This makes the two classes of experiments sensitive to different SM extensions. Although constraints on T -violating, P -conserving interactions can be derived from EDM measurements, these constraints may be model dependent (114), and EDM and neutron decay searches for T violation are complementary in some aspects.

3.4. D - and R -Coefficient Measurements

In the last decade, there have been two major experimental efforts, EMI T and Trine, to improve the limit on the D coefficient in neutron decay. Each requires an intense, longitudinally polarized beam of cold neutrons around which one places alternating proton and electron detectors. Coincidence data are collected in electron-proton pairs as a function of the neutron spin state to search for the triple correlation.

In the EMI T experiment, the detector consisted of four electron detectors and four proton detectors arranged octagonally around the neutron beam (115). The octagonal geometry maximized the experiment's sensitivity to D by balancing the sine dependence of the cross product $\sigma_n \cdot \vec{p}_e \times \vec{p}_p$ with the large angles between the proton and electron momenta that are favored by kinematics. The decay protons drifted in a field free region before being focused by a 30 kV to 37 kV potential into an array of PIN (positive-intrinsic-negative) diode detectors. With its maximum recoil energy of 750 eV, most of the protons arrived approximately 1 μ s after the electrons. Detector pairs were grouped in the analysis to reduce potential systematic effects from neutron transverse polarization. The result from the first run of EMI T yielded an improved limit of $D = [-0.6 \pm 1.2(\text{stat}) \pm 0.5(\text{sys})] \times 10^{-3}$ (115).

Currently, the best constraint on D comes from the Trine collaboration, which reports $D = [-2.8 \pm 6.4(\text{stat}) \pm 3.0(\text{sys})] \times 10^{-4}$ (116). They used two proton detectors and two electron detectors in a rectangular geometry. The proton detectors were comprised of arrays of thin-window, low-noise PIN diodes. The detectors were held at ground while the neutron beam was set to a potential of 25 kV by surrounding it with a high voltage electrode; the field was shaped to focus the decay protons onto the PIN arrays. The electrons were detected by plastic scintillators in coincidence with multi-wire proportional chambers. This coincidence provides reduction in the gamma-ray background rates and positional information on the decay, thus minimizing some sources of systematic uncertainty.

With the current PDG limit and the Trine result, one obtains a new value for the neutron D coefficient of $(-3.9 \pm 5.9) \times 10^{-4}$, which constrains the phase of g_A/g_V to $180.05^\circ \pm 0.08^\circ$. Neither experiment produced a statistically limited result, and both collaborations upgraded their detectors and performed second runs (117, 118). In the near future it is reasonable to anticipate new results that will

put a limit on D very near 10^{-4} . Although there have been discussions and ideas for experiments using UCNs, there are currently no concrete proposals to further improve the limit on D .

Another T -odd correlation that may be present in neutron decay is the R correlation, $R\vec{\sigma} \cdot (\vec{\sigma}_e \times \vec{p}_e)$, where σ is the neutron spin and $\vec{\sigma}_e$ is the spin of the decay electron. A nonzero R requires the presence of scalar or tensor couplings and is sensitive to different SM extensions than D . An effort is underway at PSI to measure R in neutron decay by measuring the neutron polarization and the momentum and transverse polarization of the decay electron at the level of 5×10^{-3} (119).

Neutron decay is a mixed Fermi and Gamov-Teller decay, so a measurement of R would produce a limit on both scalar and tensor T -odd couplings. The limit on R achieved in ${}^8\text{Li}$ Gamov-teller decay of $R = (0.9 \pm 2.2) \times 10^{-3}$ now sets the most stringent limits for time-reversal violating tensor couplings in semileptonic weak decays, $-0.022 < \text{Im}(C_T + C'_T)/C_A < 0.017$ (120).

3.5. T -Violation in Neutron Optics

T violation can lead to terms in the forward scattering amplitude for polarized neutrons in polarized or aligned targets of the form $\vec{s} \cdot (\vec{k} \times \vec{I})$ and the fivefold correlation $\vec{s} \cdot (\vec{k} \times \vec{I})(\vec{k} \cdot \vec{I})$ (121), where \vec{s} is the neutron spin and \vec{I} is the nuclear polarization. Because the enhancement mechanisms for parity violation in compound resonances of heavy nuclei are also applicable to T -odd interactions (122) (see Section 4), it is possible for such searches to reach interesting levels of sensitivity. Although in principle T -odd observables in forward scattering are motion-reversal invariant and therefore not subject to final state effects, in practice the large spin dependence of the neutron-nucleus strong interaction in a polarized target can induce large potential sources of systematic errors which require careful study.

These systematic effects are smaller in aligned targets, and a search for the fivefold correlation in MeV polarized neutron transmission in an aligned holmium target has set the best direct limit on such interactions (123). This P -even, T -odd correlation is especially interesting, because there exist no renormalizable gauge theories with P -even T -odd tree-level gauge boson couplings between quarks (124). Although EDM limits can also be used to constrain P -even T -odd interactions in many models, in general only direct measurements can set model-independent bounds (125). Searches for the threefold P -odd T -odd correlation require a polarized target. Nuclei have been identified (${}^{139}\text{La}$, ${}^{131}\text{Xe}$) that are polarizable in macroscopic quantities and possess large parity-odd asymmetries at low energy p-wave resonances (126–128). The first steps toward such an experiment are in progress at KEK (129). A JINR-ITEP (Institute for Theoretical and Experimental Physics) collaboration is also preparing to perform a search for the P -even T -odd fivefold correlation with low energy neutrons on p-wave resonances using microwave-induced dynamical nuclear alignment to order the nuclei (130, 131).

3.6. Neutron-Antineutron Oscillations

An observation of neutron-antineutron oscillations would constitute a discovery of fundamental importance (132). The existence of such an effect requires a change of baryon number by 2 units and no change in lepton number and therefore must be mediated by an interaction outside the SM of particle physics. Among neutral mesons and leptons with distinct particle and antiparticle species and sufficiently long lifetimes (neutrinos, kaons, B mesons), oscillations are no longer a surprising phenomenon. The observation of oscillations in these systems has yielded information on aspects of physics (lepton number violation, T violation, neutrino mass) that are not accessible using less sensitive techniques. It is reasonable to hope that a search for oscillations in the neutron, the only neutral baryon which is sufficiently long-lived to conduct a practical experiment, may uncover new processes in nature.

In the SM there are no renormalizable interactions one can write down which violate B , and any nonrenormalizable operator that can induce B violation must be suppressed by some heavy mass scale. The effective operator for neutron-antineutron oscillations involves a dimension 9 operator to change the 3 quarks in the neutron into 3 antiquarks and is suppressed by some mass scale to the 5th power. Some SM extensions lead to B violation by 2 units and not 1 unit. Examples include left-right symmetric models (133) with a local $B-L$ symmetry needed to generate small Majorana neutrino masses by the seesaw mechanism, SUSY models with spontaneously broken $B-L$ symmetry (134), and theories with compactified extra dimensions which attempt to solve hierarchy problems by introducing a much lower scale (TeV) for the onset of quantum gravity (135). In these cases proton decay is unobservably small but neutron-antineutron oscillations can occur close to the present limit. A general analysis of all operators with scalar bilinears that couple to two SM fermion fields uncovers operators that can only lead to neutron-antineutron oscillations and not to proton decay (136).

The last experiment in the free neutron system at the ILL set an upper limit of 8.6×10^7 s (90% confidence level) on the oscillation time (137). Translated into a mass scale, this limit excludes mass scales for the effective operator that induces oscillations below ~ 100 TeV. A similar indirect limit is set by the absence of evidence for spontaneous neutron-antineutron oscillations in nuclei in large underground detectors built for proton decay and neutrino oscillation studies (138). Although there has been some discussion of possible strategies to improve on the bounds from direct searches using cold and ultracold neutrons (139, 140), there are no new free neutron-antineutron oscillation searches underway.

4. NEUTRON-NUCLEON WEAK INTERACTIONS

The most obvious consequence of the weak interaction for neutrons is that it makes neutrons unstable. In addition to the coupling of quarks to leptons that allows neutrons to decay, electroweak theory also predicts (and experiments confirm)

that there are weak interactions between the quarks in the neutron with couplings comparable in size to those involved in neutron decay. The weak nucleon-nucleon (NN) interaction is a unique probe of strongly interacting systems. This section presents an overview of the importance of NN interactions for QCD and the status of the experimental efforts. Reviews of aspects of the field can be found in References (141–143).

4.1. Overview

The dynamics of the quarks in the nucleon are dominated by momentum transfers that are less than that set by the QCD scale of $1 \text{ GeV}/c$. In this regime QCD becomes so strong that quarks are permanently confined, and therefore the quark-quark weak interactions appear through the NN weak interactions that they induce. At these energies quark-quark weak amplitudes are of order 10^{-7} of strong amplitudes primarily because of the short range of the quark weak interactions through W and Z exchange.

Assuming that it is correctly described by the electroweak theory at low energy scales, the quark-quark weak interaction can be viewed as an internal probe of strongly interacting systems. Collider measurements have verified the SM predictions for quark-quark weak couplings for large momentum transfers at the 10% level (144). The interaction is too weak to significantly affect the strong dynamics or to excite the system, and therefore it probes quark-quark correlations in the QCD ground state. The effects of the quark-quark weak interaction can be isolated from the strong interaction using parity violation. The short range of the quark-quark weak interaction and its ability to violate parity make it visible and sensitive to interesting aspects of strongly interacting systems, as seen in four cases.

1. The ground state of the strongly interacting limit of QCD is a problem of fundamental importance. Although the dynamics that lead to the spontaneous breakdown of chiral symmetry in QCD are not yet understood, one of the leading models assumes the importance of fluctuating nonperturbative gluon field configurations called instantons (145). They induce four-quark vertices that flip the quark helicity and localize the quark wave function through a mechanism similar to Anderson localization of electrons in disordered metals (146). Some aspects of QCD spectroscopy and the high density limit can be understood by assuming that quark-diquark configurations in the nucleon are important (147). The mechanism for the phenomenon of color superconductivity in the high density limit of QCD consists of a BCS-like condensation of diquarks (148). The quark-quark weak interaction in the nucleon in the low energy limit induces four-quark operators with a known spin and flavor dependence whose relative sizes are in principle sensitive to these and other correlation phenomena in the ground state of QCD.
2. With experimental information on the low energy parity-violating (PV) partial waves in the NN system, there is a chance to understand quantitatively for the first time the extensive observations performed in many systems of

PV phenomena in nuclei (149). Nuclear parity violation is linearly sensitive to small components of the nuclear wavefunction because successive shell model levels alternate in parity, and parity-odd operators directly connect adjacent shells (150). Ideas from quantum chaos (151) and nuclear statistical spectroscopy have been used to analyze parity violation in neutron reactions in heavy nuclei in terms of the effective isovector and isoscalar weak NN interaction, and knowledge of PV in the NN system would allow a quantitative test of the predictive power of these ideas (152, 153). The matrix elements for weak NN interactions in nuclei also bear many similarities to the types of matrix elements that must be calculated to interpret limits on neutrino masses from double beta decay searches (154).

3. In atoms, the effect of NN parity violation was seen for the first time in ^{133}Cs (155) through its contribution to the anapole moment of the nucleus, which is an axial vector coupling of the photon to the nucleus induced mainly by the PV NN interaction (156, 157). Anapole moment measurements in other atoms are possible, and experiments are in progress (158). In heavy nuclei for which the anapole moment is a well-defined observable, the main contribution comes from PV admixtures in the nuclear ground state wave function (159). In electron scattering from nucleons, PV effects are sensitive to both Z exchange between the electron and the quarks in the nucleon as well as the coupling of the virtual photon to the axial current from PV interactions among the quarks in the nucleon. As PV effects in electromagnetic processes are used to learn about the nucleon (160), it will be important to know enough about the weak NN interaction to extract the information of interest.
4. The NN weak interaction is also the only practical way to study quark-quark neutral currents at low energy. The neutral weak current conserves quark flavor to high accuracy in the standard electroweak model (due to the GIM mechanism) and is not seen at all in the well-studied strangeness-changing nonleptonic weak decays. We know nothing experimentally about how QCD modifies weak neutral currents.

There are theoretical difficulties in trying to relate the underlying electroweak currents to low-energy observables in the strongly interacting regime of QCD. One expects the strong repulsion in the NN interaction to keep the nucleons sufficiently separated for a direct exchange of W and Z bosons between quarks to represent an accurate dynamical mechanism. If one knew weak NN couplings from experiment, they could be used to interpret parity violation effects in nuclei. The current approach is to split the problem into two parts. The first step maps QCD to an effective theory expressed in terms of the important degrees of freedom of low energy QCD, mesons and nucleons. In this process, the effects of quark-quark weak currents appear as PV meson-nucleon couplings (161). The second step uses this effective theory to calculate electroweak effects in the NN interaction in terms of weak couplings. The couplings themselves also become challenging targets for calculation from the SM.

4.2. Theoretical Description

In the work of Desplanques, Donoghue, and Holstein (DDH) (161), the authors used a valence quark model in combination with SU(6) symmetry relations and data on hyperon decays to produce a range of predictions for effective PV meson-nucleon couplings from the SM. At low energy, the weak interaction between nucleons in this approach is parameterized by the weak pion coupling constant f_π , and six other meson coupling denoted as $h_\rho^0, h_\rho^1, h_\rho^{1'}, h_\rho^2, h_\omega^0$, and h_ω^1 , where the subscript denotes the exchanged meson and the superscript indicates the isospin change. Due to uncertainties in the effects of strong QCD, the range of predictions for the size of these weak couplings is rather broad. For the weak pion coupling, neutral currents should play a dominant role. Another strategy is to perform a systematic analysis of the weak NN interaction using an effective field theory (EFT) approach to classify the interaction in a manner that is consistent with the symmetries of QCD and does not assume any specific dynamical mechanism. Such an EFT approach has recently appeared (162). Preparations have also been made for an eventual calculation of the weak NN interaction vertices using lattice gauge theory in the partially quenched approximation (163).

At the low energies accessible with cold neutrons with $k_n R_{strong} \ll 1$, parity-odd effects in the two-nucleon system can be parameterized in terms of the five independent amplitudes for $S - P$ transitions involving the following nucleons and isospin exchanges: $^1S_0 \rightarrow ^3P_0$ (p-p, p-n, n-n, $\Delta I = 0, 1, 2$), $^3S_1 \rightarrow ^1P_1$ (n-p, $\Delta I = 0$), and $^3S_1 \rightarrow ^3P_1$ (n-p, $\Delta I = 1$). Thus, from the point of view of a phenomenological description of the weak NN interaction, at least five independent experiments are required. The PV longitudinal analyzing power in p-p scattering, which determines a linear combination of the $^1S_0 \rightarrow ^3P_0$ amplitudes, has been measured at 15 MeV and 45 MeV in several experiments with consistent results (164–167) and remains the only nonzero observation of parity violation in the pure NN system dominated by p-waves.

Parity violation in few-nucleon systems should be cleanly interpretable in terms of the NN weak interaction due to recent theoretical and computational advances for the strong interaction in few nucleon systems (168). Weak effects can be included as a perturbation. These calculations have recently been done for n-p and p-p parity violation (169–171) and can be done in principle for all light nuclei. It is also possible that these microscopic calculations can be applied to systems with somewhat larger A , such as ^{10}B and ^6Li , where measurements of P -odd observables with low energy neutrons have reached interesting levels of sensitivity (172, 173).

The longest-range part of the interaction is dominated by the weak pion-nucleon coupling constant f_π . f_π has been calculated using QCD sum rules (174) and in a SU(3) Skyrme model (175). Measurements of the circular polarization of photons in the decay of ^{18}F (176, 177) provide a value for f_π that is considerably smaller than the DDH best value though still within the reasonable range. A precision atomic physics measurement of the ^{133}Cs hyperfine structure (anapole moment) has been analyzed to give a constraint on f_π and the combination $(h_\rho^0 + 0.6h_\omega^0)$.

This result would seem to favor a value for f_π that is larger than the ^{18}F result. Figure 4 presents an exclusion plot that summarizes the current situation.

4.3. Parity-Odd Neutron Spin Rotation and Capture Gamma Asymmetries

There are a few general statements that apply to the low energy weak interactions of neutrons with low A nuclei. In the absence of resonances, the PV helicity dependence of the total cross section vanishes if only elastic scattering is present, and both the PV neutron spin rotation and the PV helicity dependence of the total cross section with inelastic channels are constant in the limit of zero neutron energy (121). These results depend only on the requirement for parity violation in an $S \rightarrow P$ transition amplitude involving two-body channels. The two practical classes of neutron experiments are PV neutron spin rotation and PV gamma asymmetries.

The NPDGamma experiment will measure the parity-violating directional gamma ray asymmetry A_γ in the capture of polarized neutrons on protons (179, 180). The unique feature of this observable is that it is sensitive to the weak pion coupling f_π , $A_\gamma = -0.11 f_\pi$ (181–183). The recently commissioned beamline at LANSCE delivers pulsed cold neutrons to the apparatus, where they are polarized by transmission through a large-volume polarized ^3He spin filter and are transported to a liquid parahydrogen target. A resonant RF spin flipper reverses the direction of the neutron spin on successive beam pulses using a sequence that minimizes susceptibility to some systematics. The 2.2 MeV gamma rays from the capture reaction are detected in an array of CsI(Tl) scintillators read out by vacuum photodiodes operated in current mode and coupled via low-noise I–V preamplifiers to transient digitizers. The current-mode CsI array possesses an intrinsic noise two orders of magnitude smaller than the shot noise from the gamma signal and has been shown in offline tests to possess no false instrumental asymmetries at the 5×10^{-9} level (184). The pulsed beam enables the neutron energy to be determined by time-of-flight, which is an important advantage for diagnosing and reducing many types of systematic uncertainty. This apparatus has been used to conduct measurements of parity violation in several medium and heavy nuclei (185).

Another experiment in preparation is a search for parity violation in neutron spin rotation in liquid ^4He (186). A transverse rotation of the neutron spin vector about its momentum manifestly violates parity (187) and can be viewed from a neutron optical point of view as due to ahelicity-dependent neutron index of refraction. For ^4He , the calculated PV neutron spin rotation in terms of weak couplings is (188)

$$\phi = (0.97f_\pi + 0.32h_\rho^0 - 0.11h_\rho^1 + 0.22h_\omega^0 - 0.22h_\omega^1) \times 10^{-6} \text{ rad/m}. \quad 4.$$

To measure the small parity-odd rotation, a neutronpolarizer-analyzer pair with axes at right angles transmitted only the component of a polarized beam that rotated as it traversed the target. The challenge was to distinguish small PV rotations from rotations that arise from residual magnetic fields. The first measurement achieved a sensitivity of 14×10^{-7} rad/m at NIST (189), and no systematic effects were seen at the 2×10^{-7} rad/m level.

Four plausible experiments employ beams of cold neutrons and involve targets with $A < 5$: measurement of the PV gamma asymmetries in $p(\bar{n}, \gamma)d$ and in $d(\bar{n}, \gamma)t$ and of the PNC neutron spin rotations in ${}^4\text{He}$ and H . Successful measurements in all of these systems, in combination with existing measurements, would have a strong impact on the knowledge of the NN weak interaction (190).

4.4. Test of Statistical Theories for Heavy Nuclei Matrix Elements

One might assume that a quantitative treatment of NN parity violation in neutron reactions with heavy nuclei would not be feasible. A low energy compound nuclear resonance expressed in terms of a Fock space basis in a shell model might possess a million components with essentially unknown coefficients, and the calculation of a parity-odd effect would involve a matrix element between such a state and another equally complicated state. However, one can imagine a theoretical approach which exploits the large number of essentially unknown coefficients in such complicated states. If we assume that it is possible to treat these components as random variables, one can devise statistical techniques to calculate, not the value of a particular parity-odd observable, but the width of the distribution of expected values. A similar strategy has been used to understand properties of complicated compound nuclear states. The distribution of energy spacings and neutron resonance widths obeys a Porter-Thomas distribution (191) in agreement with the predictions of random matrix theory, and statistical approaches have been used to understand isospin violation in heavy nuclei (192). Statistical analyses have been applied to an extensive series of measurements of parity violation in heavy nuclei performed mainly at JINR, KEK, and LANSCE (193, 194).

The TRIPLE collaboration at LANSCE measured 75 statistically significant PV asymmetries in several compound nuclear resonances in heavy nuclei. In the case of parity violation in compound resonances in neutron-nucleus reactions there are amplification mechanisms which can enhance parity-odd observables by factors as large as 10^5 . These amplification mechanisms, which are interesting phenomena in themselves, depend in an essential way on the complexity of the states involved. Part of the amplification comes from the decrease in the spacing between levels as the number of nucleons increases, which brings opposite parity states closer together and increases their weak mixing amplitudes (195, 196); for low energy neutron reactions in heavy nuclei, it leads to a generic amplification of order 10^2 in parity-odd amplitudes. In addition, for low energy neutron-nucleus interactions the resonances are mainly $l = 0$ and $l = 1$, with the scattering amplitudes in s-wave resonances larger than for p-wave resonances by a factor of order 10^2 to 10^3 . At an energy close to a p-wave resonance, the weak interaction mixes in an s-wave component that is typically much larger, and this factor amplifies the asymmetry. These amplification mechanisms were predicted theoretically (197) before they were measured (198, 199).

A basic tenet of the statistical approach is that there should be, on average, equal numbers of negative and positive PV asymmetries in a given nucleus. This

condition appears to be satisfied provided that one removes the ^{232}Th data, wherein all ten measured parity-odd asymmetries have the same sign. At present, this result is ascribed to some poorly understood nuclear structure effect. Its observation illustrates the potential for the use of NN parity violation to discover unsuspected coherent effects in complicated many-body systems.

The values of the weak matrix elements determined by the statistical analysis varied in the range 0.5 meV to 3.0 meV, in rough agreement with theory. The accuracy of this analysis was improved through new measurements of the required spectroscopic information on compound nuclear levels (200). Theoretical calculations that use this data to extract the weak isoscalar and isovector couplings in ^{238}U obtain results in qualitative agreement with DDH expectations (153). If the weak NN couplings were known, we would be able to see if there is any evidence for nuclear medium effects.

4.4.1. PARITY-ODD AND TIME REVERSAL-ODD CORRELATIONS IN NEUTRON-INDUCED TERNARY FISSION An example where symmetry violation in neutron-induced reactions has led to progress in the understanding of many-body nuclear dynamics is fission. *P*-odd effects in binary fission induced by polarized neutron capture have been observed for a long time (201, 202). Although one might expect that a treatment of parity violation in nuclear fission would be even more difficult than for compound nuclear resonances in heavy nuclei, there is a compelling understanding of parity-odd asymmetries observed in fission after capture by polarized neutrons (201–203) based on interference of amplitudes of opposite parity from parity doublets in the cold pear-shaped transition states of open channels. Since this interference occurs among the small number of fission channels in the initial state near the saddle point, it can survive the inevitable averaging over the enormous number of final states later produced in the rupture.

In the case of ternary fission, wherein a third light-charged particle (usually an alpha) is emitted in addition to the two main fragments, recent parity violation measurements have given support to a specific mechanism for the emission of the ternary particle (204). Consider two generic mechanisms for the emission of the ternary particle: the simultaneous emission of the three particles (three-body compound nucleus decay) and “double neck rupture” in which the ternary particle is emitted after the first rupture of the neck from its remnants. In the first case, because all three objects originate from the same system where the dominant parity violation comes from the mixing of opposite parity compound nuclear states, one expects all of the PV asymmetries in various channels to be about the same size. In the second case, however, the mechanism for the emission of the ternary particle does not possess the same intermediate states that are known to exist in binary fission, and upon averaging over the large number of fragment states one would expect the parity-odd correlations that involve the ternary particle to be much smaller. This is what was observed experimentally in ^{233}U (205–209). Furthermore, the parity-odd asymmetries of the two large fragments were seen to be independent of the energy of the ternary particle. Since different ternary particle

energies are presumably coming from different Coulomb repulsion effects from different shapes of the neck, this independence would also seem to indicate that the parity-odd asymmetry is established before the scission process.

In ternary fission one can also look for a T -odd triple correlation between the momenta of the light fragment and ternary particle and the neutron spin. This measurement has recently been done (210, 211) and a large nonzero effect of order 10^{-3} was seen in both ^{233}U and ^{235}U for both alphas and tritons as the ternary products. It is believed that in the ternary fission system, this correlation is due to a final state effect and not to a fundamental source of T violation. The fact that the size of the observed triple correlation depends on the ternary particle energy also suggests that a final state effect is responsible. One model (212, 213) can reproduce the order of magnitude of the effect if one assumes that the projection of the orbital angular momentum of the recoiling ternary particle changes the spin projections and therefore the level densities of the larger fragments. If the emission probabilities of the ternary particle are proportional to these level densities and the angular momentum of the initial system is correlated with the neutron polarization, this mechanism can generate a nonzero triple correlation. Semiclassically this can be viewed in terms of the Coriolis interaction of the ternary particle with the rotating compound nucleus (214). Future work will attempt to confirm this mechanism in plutonium.

5. LOW ENERGY QCD TESTS

One of the long-term goals of strong interaction physics is to see how the properties of nucleons and nuclei follow from QCD. For nuclei the first step in this process is to see if one can start from QCD and calculate the well-measured NN strong interaction scattering amplitudes and the properties of the deuteron. During the last decade a number of theoretical developments have started to show the outlines of how this connection between QCD and nuclear physics can be made. In this section, we discuss some of the theoretical developments in few nucleon systems along with several precision scattering length experiments. The status of two fundamental properties of the neutron, its polarizability and the neutron-electron scattering length, are also discussed.

5.1. Theoretical Developments in Few Nucleon Systems and the Connection to QCD

Based on a suggestion by Weinberg (215), one strategy to develop an effective field theory (216) for QCD that is valid in the low energy limit relevant for nuclei and incorporates the most important low energy symmetry of QCD is through chiral symmetry. This alone is not enough because some of the important energy scales of nuclear physics, such as the deuteron binding energy and its correspondingly large low energy scattering lengths, seem to be the result of a delicate cancellation between competing effects which will need more than chiral symmetry alone to

understand. Recent efforts to understand the emergence of smaller energy scales in nuclear physics not set by chiral dynamics have led to interesting suggestions that the low energy limit of QCD is not described by the usual renormalization group fixed point but rather is close to a limit cycle which can be reached by a fine tuning of the values of the current quark masses in the Lagrangian (217, 218).

Recently, significant insight into certain features of few nucleon systems has come from the EFT approach based on the chiral symmetry of QCD (219–221). The value of the EFT approach is that it is a well-defined field theoretical procedure for the systematic construction of a low energy Lagrangian consistent with the symmetries of QCD. To a given level of accuracy the Lagrangian contains all possible terms accompanied by symmetries with a number of arbitrary coefficients which, once fixed by experiment, can be used to calculate other observables. EFTs based on the chiral symmetry of QCD have been used to develop an understanding for the relative sizes of many quantities in nuclear physics, such as that of nuclear N -body forces (222) and in particular the nuclear three-body force (3N), which is the subject of much activity. Although it is well understood that 3N forces must exist with a weaker strength and shorter range than the NN force, little else about them is known.

EFT has been used to solve the two- and three-nucleon problems with short-range interactions in a systematic expansion of the small momentum region set by $kb \leq 1$, where k is the momentum transfer and b is the bound scattering length (163, 221). For the two-body system, EFT is equivalent to effective range theory and reproduces its well-known results for NN forces (223–225). The chiral EFT expansion does not require the introduction of an operator corresponding to a 3N force until next-to-next-to leading order in the expansion, and at this order it requires only two low energy constants (226, 227). Significant advances have been made in other approaches to the computation of the properties of few-body nuclei with modern potentials (228) such as the AV18 potential (168, 229), which includes electromagnetic terms and terms to account for charge-independence breaking and charge symmetry breaking.

All of these developments show that precision measurements of low energy strong interaction properties, such as the zero energy scattering lengths and electromagnetic properties of small A nuclei, are becoming more important for strong interaction physics both as precise data that can be used to fix parameters in the EFT expansion and also as new targets for theoretical prediction. It is possible now to envision the accurate calculation of low energy neutron scattering lengths for systems with $A > 2$.

5.2. Precision Scattering Length Measurements Using Interferometric Methods

In parallel with these theoretical developments, two interferometric methods have been perfected to allow high-precision measurements of n - A scattering lengths. One is neutron interferometry using diffraction from perfect silicon crystals (5),

which measures the coherent scattering length. The other is pseudomagnetic precession of polarized neutrons in a polarized nuclear target, which measures the incoherent scattering length. Together these two measurements can be used to determine the scattering lengths in both channels.

Neutron interferometry can be used to measure the phase shift caused by neutron propagation in the optical potential of a medium. For a target placed in one arm of an interferometer, the phase shift is given by the expression $\phi = bND\lambda$, where N is the target density, D is the thickness of the sample, λ is the neutron de Broglie wavelength, and b is the bound coherent scattering length. High absolute accuracy in the determination of N , D , and λ are required but possible at the 10^{-4} level. Recent results from measurements at the NIST Neutron Interferometry and Optics Facility yielded the coherent scattering lengths $b_{np} = (-3.738 \pm 0.002)$ fm, $b_{nd} = (6.665 \pm 0.004)$ fm (230, 231), and $b_{n^3He} = (5.857 \pm 0.007)$ fm (232). These experiments showed that almost all existing theoretical calculations of the n-d and n- ^3He coherent scattering lengths are in disagreement with experiment and that the accuracy of present measurements is sensitive to such effects as nuclear three-body forces and charge symmetry-breaking (233, 234).

If the neutron-nucleus interaction is spin dependent, a polarized neutron moving through a polarized medium possesses a contribution to the forward scattering amplitude proportional to $(b_+ - b_-)\vec{\sigma}_n \cdot \vec{I}$ where b_+ and b_- are the scattering lengths in the two channels, $\vec{\sigma}_n$ is the neutron spin, and \vec{I} is the nuclear polarization. The angle of the polarization of a neutron polarized normal to the target polarization precesses as it moves through the medium. This phenomenon is referred to as nuclear pseudomagnetic precession (235) and has been used to measure scattering length differences in many nuclei. Recently, a high-precision measurement of this precession angle was performed in polarized ^3He using a neutron spin-echo spectrometer at the ILL (236). A new experiment to determine the spin-dependence of the n-d scattering length is in preparation at PSI (237).

In combination with the n-D coherent scattering length determined by neutron interferometry, this experiment should determine both n-D scattering lengths to 10^{-3} accuracy. The $^2\text{S}_{1/2}$ scattering length in the n-d system is especially interesting. The quartet s-wave scattering length ($^4\text{S}_{3/2}$) can be unambiguously determined from current theory. Because the three nucleons in this channel exist in a spin-symmetric state, and hence have an antisymmetric space-isospin wavefunction, the scattering in this state is completely determined by the long range part of the triplet s-wave NN interaction in the n-p channel, i.e., by n-p scattering and the properties of the deuteron. By contrast the Pauli principle does not deter the doublet channel from exploring the shorter-range components of the NN interaction, where 3N forces should appear.

Perhaps the single most interesting scattering length to measure is the neutron-neutron scattering length a_{nn} . No direct measurements exist. An experiment to determine a_{nn} by viewing a high-density neutron gas near the core of a reactor and measuring a quadratic dependence of the neutron fluence on source power is currently being designed (239). An experiment to let the neutrons in an extracted

beam scatter from each other has been considered (238). The motivation for such a measurement might increase if low energy effective field theories of QCD are able to predict a_{nn} accurately. An EFT analysis to extract a_{nn} from the $\pi^- d \rightarrow nn\gamma$ reaction has recently appeared (240).

5.3. Neutron-Electron Interaction

Although the neutron has a net zero electric charge, it is composed of charged quarks which possess a nontrivial radial charge distribution. This distribution produces a nonzero value of the neutron mean-square charge radius $\langle r_n^2 \rangle$. To the first order in the electromagnetic coupling α , the neutron-electron scattering length

$$a_{ne} = \frac{2\alpha m_n c}{\hbar} \frac{dG_{eN}}{dq^2} \quad 5.$$

is proportional to the slope of the electric form factor of the neutron, G_{eN} , in the $q^2 \rightarrow 0$ limit, where q is the momentum transfer. For the proton (neutron), this limiting value for the electric form factor is normalized to one (zero). This leads to $G_{eN}(-q^2) \rightarrow \frac{1}{6}\langle r_n^2 \rangle q^2$, where $-q^2 = \vec{q}^2$ is the four-momentum transfer. Although defined for arbitrary q^2 , in the Breit frame G_{eN} has an interpretation as the spatial Fourier transform of the charge distribution of the neutron (241).

The sign of this slope, or equivalently the sign of the charge radius, has physical significance. For the neutron one expects a negative charge radius from its virtual pion cloud (242). From the QCD point of view, the neutron charge radius is especially interesting because it is more sensitive to sea quark contributions than the proton charge radius, which has a large valence quark contribution. With the advent of improved lattice gauge theory calculations of nucleon properties (243) and the ability to use chiral extrapolation procedures to ensure proper treatment of the nonanalytic chiral corrections (244), it is possible that the neutron-electron scattering length may be calculable in the near future directly from QCD.

There are two clusters of values in a_{ne} measurements. One set comes from measurements of the asymmetric angular distribution of neutron scattering in noble gases, $a_{ne} = (-1.33 \pm 0.03) \times 10^{-3}$ fm (245), and the total cross section of lead, $a_{ne} = (-1.33 \pm 0.03) \times 10^{-3}$ fm (246). The other set comes from measurements of the total cross section of bismuth, $a_{ne} = (-1.55 \pm 0.11) \times 10^{-3}$ fm (247), and neutron diffraction from a tungsten single crystal, $a_{ne} = (-1.60 \pm 0.05) \times 10^{-3}$ fm (248). Two new experiments are in preparation; one exploits dynamical diffraction in a perfect silicon crystal (F.E. Wietfeldt, personal communication), and a second attempts to improve on the technique of scattering in noble gases (249). An experiment using Bragg reflections in perfect silicon crystals to determine a_{ne} has also been proposed (250).

The precision of the charge radii of the proton and the deuteron has greatly improved during the last decade from theoretical and experimental advances

in electron scattering and atomic physics. The charge radius of the proton is well-determined from both electron scattering data, $\sqrt{r_p^2} = (0.895 \pm 0.018)$ fm (251), and from high precision atomic spectroscopy in hydrogen, $\sqrt{r_p^2} = (0.890 \pm 0.014)$ fm (252). The charge radius of the deuteron is also well-determined from electron scattering data $\sqrt{r_d^2} = (2.128 \pm 0.011)$ fm (253), a value consistent with theoretical calculations of deuteron structure from the deuteron wave function and the triplet n-p scattering length ($\sqrt{r_d^2} = 2.131$ fm) (254) and from high-precision atomic spectroscopy measurements of the $2P$ - $2S$ transition in deuterium ($\sqrt{r_p^2} = (2.133 \pm 0.007)$ fm) (255). Atomic physics measurements of the H-D isotope shift of the $1S$ - $2S$ two-photon resonance were used to derive an accurate value for the difference between the mean-square charge radii of the deuteron and proton of $r_d^2 - r_p^2 = (3.8212 \pm 0.0015)$ fm² (256). Because the neutron charge radius is simply related to the proton and deuteron charge radii, it is very timely for a theoretical analysis that uses these precise values as input and predicts the neutron mean-square charge radius in an EFT analysis.

5.4. Neutron Polarizability

The electric and magnetic polarizabilities of the neutron are fundamental properties which characterize how easily the neutron deforms under external electromagnetic fields. The quarks in the neutron are confined by the strong interaction with a tension equivalent to about one ton over their distance of separation of one fermi, so the polarizabilities are very small. To measure neutron polarizability, one may exploit the electric fields accessible on the surface of heavy nuclei which polarize the neutron to give a calculable contribution to the neutron-nucleus scattering length with a linear dependence on the neutron momentum k . A measurement using ^{208}Pb observed a term whose size and neutron energy dependence was consistent with a nonzero polarizability of $\alpha_n = [12.0 \pm 1.5(\text{stat}) \pm 2.0(\text{sys})] \times 10^{-4}$ fm³ (257). Subsequent analyses assert that the data analysis is not definitive (258–260). Another approach using deuteron Compton scattering gave $\alpha_n = [8.8 \pm 2.4(\text{stat} + \text{sys}) \pm 3.0(\text{theo})] \times 10^{-4}$ fm³ (261) whereas quasi-free Compton scattering from the deuteron gave $\alpha_n = [12.5 \pm 1.8(\text{stat})_{-0.6}^{+1.1}(\text{sys}) \pm 1.1(\text{theo})] \times 10^{-4}$ fm³ (262). The theoretical uncertainties come from different treatments of strong interaction effects.

QCD effective field theory is developing into a quantitative theory for the calculation of low energy nucleon properties. The lowest-order prediction of chiral perturbation theory for the neutron polarizability is $\alpha_n = 12.2 \times 10^{-4}$ fm³ (263), and analysis of the extensive new Compton scattering data on the proton and deuteron using an EFT analysis is in progress (264). The result should be a sharp prediction for the neutron electric polarizability from QCD. Lattice gauge theory calculations of the polarizability are improving (265). This work should motivate further efforts to improve the neutron polarizability measurement.

6. NEUTRONS IN ASTROPHYSICS AND GRAVITY

This section discusses some of the ways in which neutrons and nuclear reactions involving neutrons play vital roles in several astrophysical processes. Neutrons play a decisive role in determining the element distribution in the universe. The decay rate of the neutron determines the amount of primordial ${}^4\text{He}$ in Big Bang theory, and neutron reactions in stars form most heavy nuclei beyond iron. In addition, one can use the fact that neutrons in the gravitational field of the Earth are sensitive to potential differences comparable to those from the strong and electromagnetic interactions as an opportunity to search for gravitational effects on an elementary particle.

6.1. Big Bang Nucleosynthesis

Neutron decay influences the dynamics of Big Bang Nucleosynthesis (BBN) through both the size of the weak interaction couplings g_A and g_V and the lifetime. The couplings determine when weak interaction rates fall sufficiently below the Hubble expansion rate to cause neutrons and protons to fall out of chemical equilibrium, which occurs on the scale of a few seconds, and thus the n/p ratio decreases as the neutrons decay. The lifetime determines the fraction of neutrons available as the universe cools, most of which end up in ${}^4\text{He}$ (266), and occurs on the scale of a few minutes. The neutron lifetime remains the most uncertain nuclear parameter in cosmological models that predict the cosmic ${}^4\text{He}$ abundance (267, 268). With the recent high-precision determination of the cosmic baryon density reported by the Wilkinson Microwave Anisotropy Probe (WMAP) measurement of the microwave background (269), there is a growing tension between the BBN prediction for the ${}^4\text{He}$ abundance, which is quite sensitive to the neutrino sector of the SM, and that inferred from observation (270). BBN calculations predicted that the number of light neutrinos that couple to the Z was about 3 before the Large Electron-Positron (LEP) storage ring measurements ended all doubt. The quantitative success of BBN is now routinely used to constrain various aspects of physics beyond the SM. The small size of the baryon density relative to the density required to close the universe is one of the observational cornerstones of the dark matter problem in astrophysics.

The main concern in deviations between BBN theory and experiment remains the astronomical determinations of the ${}^4\text{He}$ abundance, whose systematic errors are perhaps not yet fully understood. As the neutron lifetime measurements improve, other neutron-induced reactions in the early universe, such as the $n + p \rightarrow d + \gamma$ cross section, will become more important to measure precisely. Some reactions that are difficult to measure would benefit from the application of EFT methods for calculation in the relevant energy regime, and again low energy neutron measurements will be useful to fix the EFT parameters. It is therefore likely that neutron measurements will continue to be relevant for BBN.

6.2. Stellar Astrophysics

An examination of the observed elemental abundances in the solar system, together with rudimentary nuclear physics considerations, reveals that neutron capture reactions are essential for the origin of the elements heavier than iron (271). Almost all these elements are thought to have been synthesized inside stars, supernovae, or other more exotic environments through sequences of neutron capture reactions and beta decays during the so-called slow neutron capture (“s”) (272) and rapid neutron capture (“r”) (273) processes. The s and r processes are each responsible for roughly half of the observed heavy element abundances. The remaining neutron-deficient isotopes that cannot be reached via neutron capture pathways are thought to have been formed in massive stars or during supernova explosions through the photodissociation (“p”) process.

In some cases, further progress in these areas is hampered by the lack of accurate rates for nuclear reactions governing stellar nucleosynthesis. Many of these astrophysical reaction rates can be determined by measuring neutron-induced cross sections in the energy range between approximately 1 eV and 300 keV. For about 20 radionuclides along the s-process path, the neutron-capture and β -decay time scales are roughly equal. The competition between neutron capture and β decay occurring at these isotopes causes branches in the s-process reaction path that, if measured, could be used to directly constrain dynamical parameters of s-process models. There is very little data on the (n,γ) reaction rates for such radioactive branching points.

Measurements of cross sections in an energy range relevant to astrophysics constitute an important program for a number of neutron beamlines at facilities such as the Oak Ridge Electron Linear Accelerator (ORELA) (274), the Geel Electron Linear Accelerator (GELINA) (275), nTOF, and the Detector for Advanced Neutron Capture Experiments (DANCE) (276), along with many others. The intensities now suffice to conduct cross section measurements on small quantities of unstable isotopes. As the understanding of the origins and processes which lead to element formation improves, we can more effectively exploit astrophysical observations to constrain the understanding of what phenomena may lie beyond the SM.

6.3. Gravitationally Induced Phase Shift

The contribution of precision neutron measurements to gravitation are few in number but notable in conceptual impact. The equivalence principle for free neutrons has been verified at the 10^{-4} level (277), and although one might do better with ultracold neutrons (278), experiments with bulk matter are several orders of magnitude more precise. Another connection between neutron physics and gravity is the observation of the gravitational phase shift by neutron interferometry, which was the first verification that the principles of quantum mechanics seem to apply to the gravitational potential as well as the potentials produced by other interactions (279, 280). This measurement has been performed with an accuracy at the 1% level, and there is a slight disagreement between theory and experiment (281).

The source of the difference is believed to lie in gravitationally induced distortions in the perfect crystal interferometer as it is rotated to change the relative height of the two paths in the interferometer. There are two plans underway, one to conduct the experiment with the interferometer suspended in a neutrally buoyant fluid to eliminate possible distortions of the interferometer crystal (H. Kaiser, personal communication) and another to use a recently developed Mach-Zehnder interferometer with cold neutrons (282).

6.4. UCN Gravitational Bound States

Experimental tests of gravity and searches for new long-range forces have attracted more interest in recent decades. A reanalysis (283) of an experiment on the principle of equivalence by Eötvös motivated a series of precise tests of the principle of equivalence culminating in the torsion balance experiments of the Eöt-Wash group, which set stringent new limits to violations of the equivalence principle (284). Recently, speculations involving the propagation of the gravitational field into extra dimensions produce as a natural consequence a modification of the inverse square law for gravity on submillimeter scales (285). Several experiments are searching for such modifications (286) and have already set useful limits. Experiments to probe extra-dimensional gravity theories using the angular and neutron energy dependence of neutron scattering from spin zero nuclei have been discussed (287).

At first glance, experiments with neutrons would not seem to offer a productive technique to conduct sensitive searches for new short-range forces of gravitational strength. Although the very small polarizability of the neutron is an advantage relative to atoms, whose van der Waals attraction poses a background issue for such searches, neutron beam densities are very small compared to bulk matter. The recent measurements in search of gravitational bound states of ultracold neutrons are of some interest for constraints on new forces at smaller distance scales (288).

For neutron kinetic energies smaller than the neutron optical potential of a plane surface, the potential seen by a neutron moving above the plane in the gravitational field of the Earth should possess neutron bound states with energies given to good approximation by the zeroes of Airy functions, which are solutions to the Schrödinger equation in a linear potential. The lowest bound state, of energy 1.4 peV, hovers above the medium at a distance of order $10 \mu\text{m}$, and any nonstandard attractive interaction of the neutron with the matter on this length scale could create another bound state.

The experiments were designed to populate these bound states by forcing the UCN to pass through a narrow gap above a planar medium and to detect their presence by measuring the transmission of the UCNs through the gap as the separation is varied. Intensity oscillations in the transmission are observed which can be fit to a model which includes the effect of the spatial extent of the bound states. The agreement of this data with theory was used to set an interesting bound on gravitational-strength forces in the nanometer range (289).

7. SUMMARY

Slow neutron experiments address fundamental scientific issues in a surprisingly large range of physics subfields. The development of new types of ultracold neutron sources, pulsed and continuous spallation sources, and the continued increase in the fluence of reactor beams are making possible new types of experiments and opening new scientific areas. We anticipate significant progress in the areas of neutron decay measurements and neutron EDM searches and also in the field of weak NN interactions and the measurement of other low energy neutron properties. We also expect more use of neutron measurements for applications in astrophysics. As is typical, many of the new opportunities made possible by technical developments and the emerging scientific issues were not clearly foreseen a decade ago. The steady progress during the last decade in quantitative theoretical understanding of the strong interaction is an underappreciated development with exciting applications to neutron physics.

Although still a relatively small field compared to other areas in nuclear and particle physics, the expanding scientific opportunities in fundamental neutron physics are attracting a growing number of young researchers. This growth is driving the increasing number and variety of new facilities. The diverse applications and the location of neutron physics at facilities whose main purpose is generally neutron scattering have combined to obscure somewhat its accomplishments. We hope that the reader has gained an appreciation for the breadth of activity in the field.

ACKNOWLEDGMENTS

We would like to thank Torsten Soldner of the ILL and Yasuhiro Masuda of KEK for their assistance in supplying some of the parameters for neutron facilities, and Scott Dewey for his careful reading of the manuscript. W.M. Snow gratefully acknowledges support from the National Science Foundation, the Department of Energy, and the Indiana 21st Century Fund. J.S. Nico acknowledges the support of the NIST Physics Laboratory and Center for Neutron Research.

**The Annual Review of Nuclear and Particle Science is online at
<http://nucl.annualreviews.org>**

LITERATURE CITED

1. Erler J, Ramsey-Musolf MJ. *Prog. Nucl. Part. Phys.* 54:351 (2005)
2. Krupchitsky PA. *Fundamental Research with Polarized Slow Neutrons*. Berlin: Springer-Verlag (1987)
3. Alexandrov Yu A. In *Fundamental Properties of the Neutron*, ed. SW Lovesey, EWJ Mitchell. Oxford: Clarendon Press (1992)
4. Byrne J. In *Neutrons, Nuclei, and Matter*. Bristol, UK: Institute of Physics Publishing (1994)
5. Rauch H, Werner S. In *Neutron Interferometry: Lessons in Experimental*

- Quantum Mechanics*, ed. SW Lovesey, EWJ Mitchell. Oxford: Oxford Univ. Press (2000)
6. Windsor CG. *Pulsed Neutron Scattering*. London: Taylor & Francis (1981)
 7. Soldner T, Nesvizhevsky V. <http://www.ill.fr/pages/science/IGroups/yb.pdf>
 8. www.frm2.tum.de/mephisto/index_en.shtml
 9. Nico JS, et al. *J. Res. Natl. Inst. Stand. Technol.* 110:137 (2005)
 10. Seo PN, et al. *Nucl. Instrum. Meth.* A517:285 (2004)
 11. Zejma J, et al. *Nucl. Inst. Meth.* A539:622 (2005)
 12. Greene GL, et al. *J. Res. Natl. Inst. Stand. Technol.* 110:149 (2005)
 13. Luschikov VI, Pokotolovsky YN, Strelkov AV, Shapiro FL. *Sov. Phys. JETP Lett.* 9:23 (1969)
 14. Steyerl A. *Phys. Lett.* B29:33 (1969)
 15. Steyerl A, et al. *Phys. Lett.* A116:347 (1986)
 16. Golub R, Pendlebury JM. *Phys. Lett.* A62:337 (1977)
 17. Ageron P, Mampe W, Golub R, Pendlebury JM. *Phys. Lett.* A66:469 (1978)
 18. Saunders A, et al. *Phys. Lett.* B593:55 (2004)
 19. Liu CY, Young AR. *Phys. Rev. B*. In press (2005)
 20. Ignatovich VK. In *The Physics of Ultracold Neutrons*, ed. SW Lovesey, EWJ Mitchell. Oxford: Clarendon Press (1990)
 21. Golub R, Richardson D, Lamoreaux SK. In *Ultra-Cold Neutrons*. Bristol, UK: Adam Hilger (1991)
 22. Byrne J. *Rep. Prog. Phys.* 45:115 (1982)
 23. Dubbers D. *Prog. Part. Nucl. Phys.* 26:173 (1991)
 24. Pendlebury JM. *Ann. Rev. Nucl. Part. Sci.* 43:687 (1993)
 25. Mund D, Abele H, eds. *Quark Mixing, CKM Unitarity*. Heidelberg: Mattes Verlag (2003)
 26. Severijns N, Beck M, Naviliat-Cuncic O. *Rev. Mod. Phys.* In press (2005)
 27. Ito TM, Prezeau G. *Phys. Rev. Lett.* 94:161802 (2005)
 28. Beck M, et al. *JETP. Lett.* 76:332 (2002)
 29. Fisher BM, et al. *J. Res. Natl. Inst. Stand. Technol.* In press (2005)
 30. Jackson JD, Treiman SB, Wyld HW. *Phys. Rev.* 106:517 (1957)
 31. Towner IS, Hardy JC. In *Symmetries and Fundamental Interactions in Nuclei*, eds. WC Haxton, EM Henley, pp. 183–249. Singapore: World Sci. (1995)
 32. Eidelman A, et al. *Phys. Lett.* B592:1 (2004)
 33. Hardy JC, Towner IS. *Phys. Rev. Lett.* 94:092502 (2005)
 34. Pocanic D, et al. *Phys. Rev. Lett.* 93:181803 (2004)
 35. Ball P, Flynn J, Kluit P, Stocchi A. In *Proceedings of the Second Workshop on the CKM Unitarity Triangle*. Durham, NC: IPPP, hep-ph/0304132 (2003)
 36. Franzini P. hep-ex/0203033
 37. Cabbibo N, Swallow E, Winston R. hep-ph/0307214
 38. Shipsey I. In *Quark Mixing, CKM Unitarity*, eds. D Mund, H Abele, pp. 175–88. Heidelberg: Mattes Verlag (2003)
 39. Spivak PE. *Zh. Eksp. Fiz.* 94:1 (1988)
 40. Mampe W, Ageron P, Bates C, Pendlebury JM, Steyerl A. *Phys. Rev. Lett.* 63:593 (1989)
 41. Nezvizhevskii VV, et al. *JETP* 75:405 (1992)
 42. Mampe W, et al. *JETP Lett.* 57:82 (1993)
 43. Byrne J, et al. *Europhys. Lett.* 33:187 (1996)
 44. Arzumanov S, et al. *Phys. Lett.* B483:15 (2000)
 45. Dewey MS, et al. *Phys. Rev. Lett.* 91:152302 (2003)
 46. Serebrov A, et al. *Phys. Lett.* B605:72 (2005)
 47. Byrne J. *Nucl. Instrum. Meth.* 284:116 (1989)
 48. Williams AP. *The Determination of the Neutron Lifetime by Trapping Decay Protons*. Ph.D. thesis. Univ. Sussex (1989)

49. Nico JS, et al. *Phys. Rev. C* 71:055502 (2005)
50. Huffman PR, et al. *Nature* 403:62 (2001)
51. Dzhosyuk SN, et al. *J. Res. Natl. Inst. Stand. Technol.* In press (2005)
52. Yerozolimsky B, et al. *J. Res. Natl. Inst. Stand. Technol.* In press (2005)
53. Picker R, et al. *J. Res. Natl. Inst. Stand. Technol.* In press (2005)
54. Liaud P, et al. *Nucl. Phys.* A612:53 (1997)
55. Schreckenbach K, et al. *Phys. Lett.* B349:427 (1995)
56. Abele H, et al. *Phys. Rev. Lett.* 88:211801 (2002)
57. Häse H, et al. *Nucl. Instrum. Meth.* A485:453 (2002)
58. Petoukhov A, et al. In *Quark Mixing, CKM Unitarity*, eds. D Mund, H Abele, pp. 123–27. Heidelberg: Mattes Verlag (2003)
59. Young AR, et al. In *Fundamental Physics with Pulsed Neutron Beams*, ed. C Gould, et al., pp. 164–80. Singapore: World Sci. (2001)
60. Serebrov AP, et al. *Nucl. Instrum. Meth.* A357:503 (1995); Zimmer O, et al. *Nucl. Instrum. Meth.* A440:764 (2000)
61. Wilburn WS, et al. In *Fundamental Physics with Pulsed Neutron Beams*, ed. C. Gould, et al. pp. 214–23. Singapore: World Sci. (2001)
62. Rich DR, et al. *Nucl. Instrum. Meth.* A481:431 (2002)
63. Jodido A, et al. *Phys. Rev. D* 34:1967 (1986)
64. Byrne J. *Europhys. Lett.* 56:633 (2001)
65. Kuznetsov IA, et al. *Phys. Rev. Lett.* 75:794 (1995)
66. Serebrov AP, et al. *JETP* 86:1074 (1998)
67. Stratowa Chr, Dobrozemsky R, Weinzierl, P. *Phys. Rev. D* 18:3970 (1978)
68. Dubbers D. *Nucl. Phys.* A527:239c (1991)
69. Yerozolimsky B, Mostovoy Y. *Sov. J. Nucl. Phys.* 53:260 (1991)
70. Gardner S, Zhang C. *Phys. Rev. Lett.* 86:5666 (2001)
71. Byrne J, et al. *J. Phys.* G28:1325 (2002)
72. Zimmer O, et al. *Nucl. Instrum. Meth.* 440:548 (2000)
73. Wietfeldt FE, et al. *Nucl. Instrum. Meth.* A545:181 (2005)
74. Yerozolimsky B. nucl-ex/0401014 (2004)
75. Baxter DB, et al. *AIP Conference Proceedings* 680:265 (2003)
76. Christenson JH, Cronin JW, Fitch VL, Turlay R. *Phys. Rev. Lett.* 13:138 (1964)
77. Alavi-Harati A, et al. *Phys. Rev. Lett.* 83:22 (1999)
78. Fanti V, et al. *Phys. Lett.* B465:335 (1999)
79. Aubert B, et al. *Phys. Rev. Lett.* 89:201802 (2002)
80. Abe K, et al. *Phys. Rev. D* 66:071102(R) (2002)
81. Herczeg P. *J. Res. Natl. Inst. Stand. Technol.* In press (2005)
82. Ramsey NF. *Ann. Rev. Nucl. Part. Sci.* 32:211 (1982)
83. Golub R, Lamoreaux SK. *Phys. Rep.* 237:1 (1994)
84. Harris PG, et al. *Phys. Rev. Lett.* 85:904 (1999)
85. Baluni V. *Phys. Rev. D* 19:2227 (1979)
86. Crewther RJ, Di Vecchia P, Veneziano G, Witten E. *Phys. Lett.* B88:123 (1979); errata 91:487 (1980)
87. Bigi II, Sanda AI. In *CP Violation*. Cambridge: Cambridge Univ. Press (2000)
88. Peccei R, Quinn H. *Phys. Rev. Lett.* 38:1440 (1977); *Phys. Rev. D* 16:1791 (1977)
89. Khriplovich IB, Zhitnitsky AR. *Phys. Lett.* B109:490 (1982)
90. Gavela MB. *Phys. Lett.* B109:215 (1982)
91. Bennett CL, et al. (WMAP Collaboration). astro-ph/0302207 (2003)
92. Sakharov AD. *JETP Lett.* 5:24 (1967)
93. Riotto A, Trodden M. *Ann. Rev. Nucl. Part. Sci.* 49:35
94. Weinberg S. In *The First Three Minutes*. New York: Harper-Collins (1977)
95. Kuzmin VA, Rubakov VA, Shaposhnikov ME. *Phys. Lett.* B155:36 (1985)
96. Shaposhnikov ME. *Nucl. Phys.* B287:757 (1987)
97. 't Hooft G. *Phys. Rev. Lett.* 37:8 (1976)

98. Cline JM. *Pramana—J. Phys.* 55:1 (2000)
99. Fukugita M, Yanagida T. *Phys. Lett.* B174:45 (1986)
100. Büchmüller W, Peccei R, Yanagida T. *Ann. Rev. Nucl. Part. Sci.* 55: (2005)
101. Dine M, Kusenko A. *Rev. Mod. Phys.* 76:1 (2004)
102. Riotto A. *Phys. Rev. D* 58:0950099 (1998)
103. Barbieri R, Romanino A, Strumia A. *Phys. Lett.* B369:283 (1996)
104. Dimopoulos S, Hall LJ. *Phys. Lett.* B344:185 (1995)
105. Khriplovich IB, Zyablyuk KN. *Phys. Lett.* B383:429 (1996)
106. Altarev IS, et al. *Phys. At. Nucl.* 59:1152 (1996)
107. Voronin VV, Lapin EG, Semenikhin S Yu, Federov VV. *JETP Lett.* 71:76 (2000)
108. Zeyen CME, Otake Y. *Nucl. Instrum. Meth.* A440:489 (2000)
109. Golub R, Lamoreaux SK. *nucl-ex/991-0001* (1999)
110. Herczeg P. *Prog. Part. Nucl. Phys.* 46:413 (2001)
111. Wenninger H, Steiwe J, Leutz H. *Nucl. Phys.* A109:561 (1968)
112. Carnoy AS, Deutsch J, Quin P. *Nucl. Phys.* A568:265 (1994)
113. Callan CG, Treiman SB. *Phys. Rev.* 162:1494 (1967)
114. Ramsey-Musolf MJ. In *Fundamental Physics with Pulsed Neutron Beams* eds. C Gould, et al., pp. 97–107. Singapore: World Sci. (2001)
115. Lising LJ, et al. *Phys. Rev. C* 62:055501 (2000)
116. Soldner T, et al. *Phys. Lett.* B581:49 (2004)
117. Mumm HP, et al. *Rev. Sci. Instrum.* 75:5343 (2004)
118. Plonka C. *Untersuchung der Zeitumkehrinvarianz am D-Koeffizienten des freien Neutronenzerfalls mit TRINE.* Ph.D. thesis. Technical Univ. Munich (2004)
119. Bodek K, et al. *J. Res. Natl. Inst. Stand. Technol.* In press (2005)
120. Huber R, et al. *Phys. Rev. Lett.* 90:202301 (2003)
121. Stodolsky L. *Nucl. Phys.* B197:213 (1982)
122. Bunakov VE, Gudkov VP. *Z. Phys. A* 308:363 (1982)
123. Huffman PR, et al. *Phys. Rev. C* 55:2684 (1997)
124. Herczeg P. *Hyperfine Interactions* 75:127 (1992)
125. Ramsay-Musolf MJ. *Phys. Rev. Lett.* 83:3997 (1999)
126. Alfimenkov VP, et al. *JETP Lett.* 34:308 (1982)
127. Szymanski JJ, et al. *Phys. Rev. C* 53:R2576 (1996)
128. Skoy VR, et al. *Phys. Rev. C* 53:R2573 (1996)
129. Masuda Y. *Nucl. Inst. Meth.* A440:632 (2000)
130. Atsarkin VA, Barabanov AL, Beda AG, Novitsky VV. *Nucl. Instrum. Meth.* A440:626 (2000)
131. Barabanov AL, Beda AG, Volkov AF. *Czech. J. Phys.* B53: 371 (2003)
132. Kuzmin VA. *JETP Lett.* 12:228 (1970)
133. Mohapathra R, Marshak R. *Phys. Rev. Lett.* 44:1316 (1980)
134. Babu KS, Mohapathra RN. *Phys. Lett.* B518:269 (2001)
135. Dvali GR, Gabadadze G. *Phys. Lett.* B460:47 (1999)
136. Klapdor-Kleingrothaus HV, Ma E, Sarkar U. *Mod. Phys. Lett.* A17:2221 (2002)
137. Baldo-Ceolin M, et al. *Z. Phys. C* 63:409 (1994)
138. Kamyshev Y, Kolbe E. *Phys. Rev. D* 67:076007 (2003)
139. Kamyshev Y. *hep-ex/0211006* (2002)
140. *International Workshop on N-Nbar Transition Search with Ultracold Neutrons.* Bloomington, IN: Indiana Univ. <http://www.iucf.indiana.edu/Seminars/NNBAR/workshop.shtml> (2002)
141. Haeblerli W, Holstein B. In *Symmetries and Fundamental Interactions in Nuclei*, eds. WC Haxton, EM Henley, pp. 17–66. Singapore: World Sci. (1995)

142. Desplanques B. *Phys. Rep.* 297:1 (1998)
143. Dmitriev VF, Khriplovich IB. *Phys. Rep.* 391:243 (2004)
144. Arnison G, et al. *Phys. Lett.* B166:484 (1986)
145. Belavin A, Polyakov A, Schwartz A, Tyupkin Yu. *Phys. Lett.* 59:85 (1975)
146. Schafer T, Shuryak E. *Rev. Mod. Phys.* 70:323 (1998)
147. Anselmino M, et al. *Rev. Mod. Phys.* 65:1199 (1993)
148. Alford M, Rajagopal K, Wilczek F. *Nucl. Phys.* B537:433 (1999)
149. Adelberger EG, Haxton WC. *Ann. Rev. Nucl. Part. Sci.* 35:501 (1985)
150. Adelberger EG. *J. Phys. Soc. Jpn.* 54:6 (1985)
151. Zelevinsky V. *Ann. Rev. Nucl. Part. Sci.* 46:238 (1996)
152. Bowman JD, Garvey GT, Johnson MB. *Ann. Rev. Nucl. Part. Sci.* 43:829 (1993)
153. Tomsovic S, Johnson MB, Hayes A, Bowman JD. *Phys. Rev. C* 62:054607 (2000)
154. Prezeau G, Ramsay-Musolf M, Vogel P. *Phys. Rev. D* 68:034016 (2003)
155. Wood CS, et al. *Science* 275:1759 (1997)
156. Zeldovich YB. *Sov. Phys. JETP* 6:1184 (1957)
157. Flambaum VV, Khriplovich IB. *Sov. Phys. JETP* 52:835 (1980)
158. Aubin S, et al. In *Proceedings of the XV International Conference on Laser Spectroscopy*, eds. S Chu, V Vuletic, AJ Kemand, C Chin, pp. 305–9. Singapore: World Sci. (2002)
159. Haxton W, Weiman CE. *Ann. Rev. Nucl. Part. Sci.* 51:261 (2001)
160. Beck DH, Holstein B. *Int. J. Mod. Phys. E* 10:1 (2001)
161. Desplanques B, Donoghue J, Holstein B. *Ann. Phys.* 124:449 (1980)
162. Zhu SL, et al. nucl-th/0407087, *Nucl. Phys.* A748:435 (2005)
163. Beane SR, Savage MJ. *Nucl. Phys.* B636:291 (2002)
164. Potter JM, et al. *Phys. Rev. Lett.* 33:1594 (1974)
165. Balzer R, et al. *Phys. Rev. Lett.* 44:699 (1980)
166. Kistryn S, et al. *Phys. Rev. Lett.* 58:1616 (1987)
167. Eversheim PD, et al. *Phys. Lett.* B256:11 (1991)
168. Pieper SC, Wiringa RB. *Ann. Rev. Nucl. Part. Sci.* 51:53 (2001)
169. Carlson J, Schiavilla R, Brown VR, Gibson BF. *Phys. Rev. C* 65:035502 (2002)
170. Schiavilla R, Carlson J, Paris M. *Phys. Rev. C* 67:032501 (2003)
171. Schiavilla R, Carlson J, Paris M. *Phys. Rev. C* 70:044007 (2004)
172. Vesna VA, et al. *Phys. At. Nucl.* 62:565 (1999)
173. Vesna VA, et al. *Izves. AN Ser. Phys.* 67:118 (2003)
174. Henley EM, Hwang WY, Kisslinger L. *Phys. Lett.* B271:403 (1998)
175. Meissner U-G, Weigel H. *Phys. Lett* B447:1 (1999)
176. Page SA, et al. *Phys. Rev. C* 35:1119 (1987)
177. Bini M, Fazzini TF, Poggi G, Taccetti N. *Phys. Rev. Lett* 55:795 (1985)
178. Haxton WC, Liu C-P, Ramsey-Musolf MJ. *Phys. Rev. Lett.* 86:5247 (2001)
179. Snow WM, et al. *Nucl. Instrum. Meth.* A440:729 (2000)
180. Snow WM, et al. *Nucl. Instrum. Meth.* A515:563 (2003)
181. Desplanques B. *Nucl. Phys.* A242:423 (1975)
182. Desplanques B. *Nucl. Phys.* A335:147 (1980)
183. Desplanques B. *Phys. Lett.* B512:305 (2001)
184. Gericke M, et al. *Nucl. Instrum Meth.* A540:328 (2005)
185. Mitchell GS, et al. *Nucl. Instrum. Meth.* A521:468 (2004)
186. Bass CD, et al. *J. Res. Natl. Inst. Stand. Technol.* 110:205 (2005)
187. Michel FC. *Phys. Rev.* 133:B329 (1964)
188. Dmitriev VF, Flambaum VV, Sushkov OP, Telitsin VB. *Phys. Lett.* B125:1 (1983)

189. Markoff DM. *Measurement of the Parity Nonconserving Spin-Rotation of Transmitted Cold Neutrons Through a Liquid Helium Target*. Ph.D. thesis. Univ. Washington (1997)
190. Snow WM. *J. Res. Natl. Inst. Stand. Technol.* 110:189 (2005)
191. Porter CE. *Statistical Theories of Spectra: Fluctuations*. New York: Academic Press (1965)
192. Harney HJL, Richter A, Weidenmuller HA. *Rev. Mod. Phys.* 58:607 (1986)
193. Mitchell GE, Bowman JD, Weidenmuller HA. *Rev. Mod. Phys.* 71:445 (1999)
194. Mitchell GE, Bowman JD, Penttila SI, Sharapov EI. *Phys. Rep.* 354:157 (2001)
195. French JB, Kota VKB, Pandey A, Tomsovic A. *Ann. Phys.* 181:198 (1988)
196. French JB, Kota VKB, Pandey A, Tomsovic A. *Ann. Phys.* 181:235 (1988)
197. Sushkov OP, Flambaum VV. *JETP Lett.* 32:352 (1980)
198. Alfimenzov VP, et al. *JETP Lett.* 35:51 (1982)
199. Alfimenzov VP, et al. *Nucl. Phys.* A398: 93 (1983)
200. Corvi F, Przytula M. *Phys. Part. Nuclei* 35:767 (2004)
201. Danilyan GV, et al. *JETP Lett.* 26:186 (1977)
202. Vodennikov BD, et al. *JETP Lett.* 27:62 (1978)
203. Shuskov OP, Flambaum VV. *Sov. Phys. Usp.* 25:1 (1982)
204. Bunakov VE, Goennenwein F. *Phys. At. Nucl.* 65:2036 (2002)
205. Petrov G, et al. *Nucl. Phys.* A502:297 (1989)
206. Belozherov AV, et al. *JETP Lett.* 54:132 (1991)
207. Goennenwein F, et al. *Nucl. Phys.* A567:303 (1994)
208. Jesinger P, et al. *Phys. At. Nucl.* 65:630 (2002)
209. Koetzle A, et al. *Nucl. Instrum. Meth.* A440:618 (2000)
210. Jesinger P, et al. *Phys. At. Nucl.* 62:1608 (1999)
211. Jesinger P, et al. *Nucl. Instrum. Meth.* A440:618 (2000)
212. Bunakov VE. *Phys. At. Nucl.* 65:616 (2002); 65:648 (2002)
213. Kadmsky SG. *Phys. At. Nucl.* 65:1785 (2002)
214. Bunakov VE, Kadmsky SG. *Phys. At. Nucl.* 66:1846 (2003)
215. Weinberg S. *Physica A* 96:327 (1979)
216. Georgi H. *Ann. Rev. Nucl. Part. Sci.* 43:209 (1993)
217. Braaten E, Hammer HW. *Phys. Rev. Lett.* 91:102002 (2003)
218. Braaten E, Hammer HW. cond-mat/0410417 (2004)
219. Bedaque PF, van Kolck U. *Phys. Lett.* B428:221 (1998)
220. Hammer HW. nucl-th/9905036 (1999)
221. Bedaque PF, van Kolck U. *Ann. Rev. Nucl. Part. Sci.* 52:339 (2002)
222. Friar J. In *Nuclear Physics with EFT*, eds. R Seki, U van Kolck, MJ Savage, pp. 145–161. Singapore: World Sci. (2001)
223. van Kolck U. *Nucl. Phys.* A645:273 (1999)
224. Kaplan DB, Savage MJ, Wise MB. *Phys. Lett.* B424:390 (1998)
225. Gegelia J. nucl-th/9802038 (1998)
226. Epelbaum E, et al. *Phys. Rev. Lett.* 86: 4787 (2001)
227. Epelbaum E, et al. *Phys. Rev. C* 66:064001 (2002)
228. Carlson J, Schiavilla R. *Rev. Mod. Phys.* 70:743 (1998)
229. Wiringa RB, Stoks VGI, Schiavilla R. *Phys. Rev. C* 51:38 (1995)
230. Black T, et al. *Phys. Rev. Lett.* 90:192502 (2003)
231. Schoen K, et al. *Phys. Rev. C* 67:044005 (2003)
232. Huffman PR, et al. *Phys. Rev. C* 70: 014004 (2004)
233. Hofmann HM, Hale GM. *Phys. Rev. C* 68:021002(R) (2003)
234. Witala H, et al. nucl/th 0305028 (2003)
235. Abragam A, et al. *Phys. Rev. Lett.* 31:776 (1973)

236. Zimmer O, et al. *EJPdirect* A1:1 (2002)
237. van der Brandt B, et al. *Nucl. Instrum. Meth.* A526:91 (2004)
238. Pokotilovskii YuN. *Phys. At. Nucl.* 56: 524 (1993)
239. Furman WI, et al. *J. Phys. G Nucl. Part. Phys.* 28:2627 (2002)
240. Gardestig A, Phillips DR. *nucl-th/0501049* (2005)
241. Isgur N. *Phys. Rev. Lett.* 83:272 (1999)
242. Hand L, Miller DG, Wilson R. *Rev. Mod. Phys.* 35:335 (1963)
243. Tang A, Wilcox W, Lewis R. *Phys. Rev. D* 68:094503 (2003)
244. Leinweber DB, Thomas AW, Young RD. *Phys. Rev. Lett.* 86:5011 (2001)
245. Krohn VE, Ringo GR. *Phys. Rev.* 148:1303 (1966); *Phys. Rev. D* 8:1305 (1973)
246. Kopecky S, et al. *Phys. Rev. C* 56: 2229 (1997)
247. Alexandrov YA, et al. *Yad. Fiz.* 44:1384 (1986)
248. Alexandrov YA, et al. *Zh. Eksp. Teor. Fiz.* 89:34 (1985)
249. Mitsyna LV, et al. In *JINR, Dubna preprint* E3-2003-183 (2003)
250. Sparenberg J-M, Leeb H. *Phys. Rev. C* 66:055210 (2002)
251. Sick I. *Phys. Lett.* B576:62 (2003)
252. Udem T, et al. *Phys. Rev. Lett.* 79:2646 (1997)
253. Sick I, Trautmann D. *Phys. Lett.* B375:16 (1996)
254. Klarsfeld S, et al. *Nucl. Phys.* A456:373 (1986)
255. Pachucki K, Weitz M, Hänsch TW. *Phys. Rev. A* 49:2255 (1994)
256. Huber A, et al. *Phys. Rev. Lett.* 80:468 (1998)
257. Schmiedmayer J, Riehs P, Harvey JA, Hill NW. *Phys. Rev. Lett.* 66:1015 (1991)
258. Koester L, et al. *Phys. Rev. C* 51:3363 (1995)
259. Aleksejeva A, et al. *Phys. Scripta* 56:20 (1997)
260. Wissmann F, Levchuk MI, Schumacher M. *Euro. Phys. J.* A1:193 (1998)
261. Lundin M, et al. *Phys. Rev. Lett.* 90: 192501 (2003)
262. Kossert K, et al. *Phys. Rev. Lett.* 88: 162301 (2002)
263. Bernard V, Kaiser N, Meissner UG. *Phys. Rev. Lett.* 67:1515 (1991)
264. Beane SR, et al. *nucl-th/0403088* (2004)
265. Christensen J, Wilcox W, Lee FX, Zhou L. *hep-lat/0408024* (2004)
266. Schramm DN, Wagoner RV. *Ann. Rev. Nucl. Part. Sci.* 27:37 (1977)
267. Lopez RE, Turner MS. *Phys. Rev. D* 59:103502-1 (1999)
268. Burles S, Nollett KM, Truran JW, Turner MS. *Phys. Rev. Lett.* 82:4176 (1999)
269. Spergel DN, et al. (WMAP collaboration). *Astrophys. J. Suppl.* 148:175 (2003)
270. Cyburt RH, Fields BD, Olive KA. *Phys. Lett.* B567:227 (2003)
271. Käppeler F, Thielemann F-K, Wiescher M. *Ann. Rev. Nucl. Part. Sci.* 48:175 (1998)
272. Kappeler F. *Prog. Part. Nucl. Phys.* 43:419 (1999)
273. Qian YZ. *Prog. Part. Nucl. Phys.* 50:153 (2003)
274. Koehler PE. *Nucl. Instrum. Meth.* A460: 352 (2001)
275. Flaska M, et al. *Nucl. Instrum. Meth.* A531:392 (2004)
276. Reifarh R, et al. *Nucl. Instrum. Meth.* A531:528 (2004)
277. Schmiedmayer J. *Nucl. Instrum. Meth.* A284:59 (1989)
278. Pokotilovskii YN. *Phys. At. Nucl.* 57:390 (1994)
279. Colella R, Overhauser AW, Werner SA. *Phys. Rev. Lett.* 34:1472 (1975)
280. Rauch H, Treimer W, Bonse U. *Phys. Lett.* A47:369 (1974)
281. Littrell KC, Allman BE, Werner SA. *Phys. Rev. A* 56:1787 (1997)
282. Funahashi H. *Nucl. Instrum. Meth.* A529: 172 (2004)
283. Fischbach E, et al. *Phys. Rev. Lett* 56:3 (1986)

-
284. Gundlach JH, et al. *Phys. Rev. Lett.* 78: 2523 (1997)
285. Sundrum R. *J. High Energy Phys.* 07:001 (1999)
286. Adelberger EG, Heckel BR, Nelson AE. *Ann. Rev. Nuc. Part. Sci.* 53:77 (2003)
287. Frank A, van Isacker C, Gomez-Camacho C. *Phys. Lett.* B582:15 (2004)
288. Nesvizhevsky VV, et al. *Nature* 415:297 (2002)
289. Nesvizhevsky VV, Protasov KV. *Class. Quant. Gravity* 21:4557 (2004)

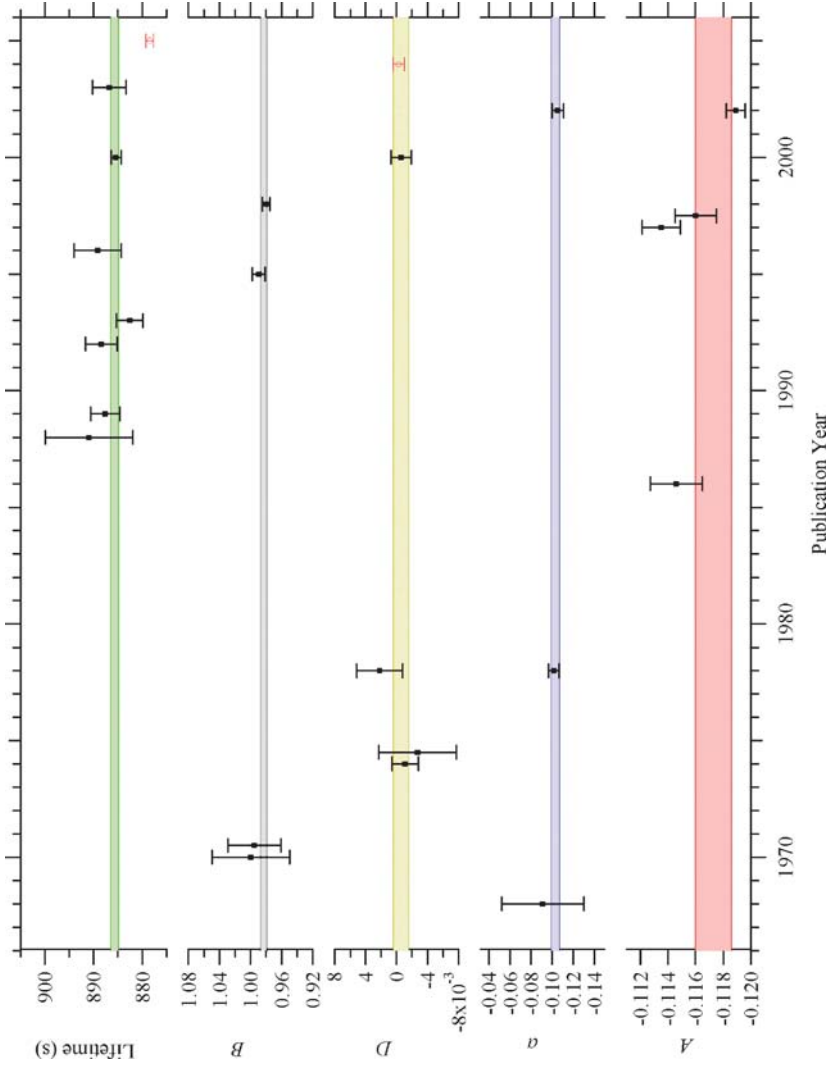


Figure 1 A summary plot of the measurements of the neutron lifetime and correlation coefficients that are used in the 2004 compilation of the Particle Data Group (PDG). Data points with open circles have not yet been included in the evaluation. The shaded bands represent the $\pm 1\sigma$ region.

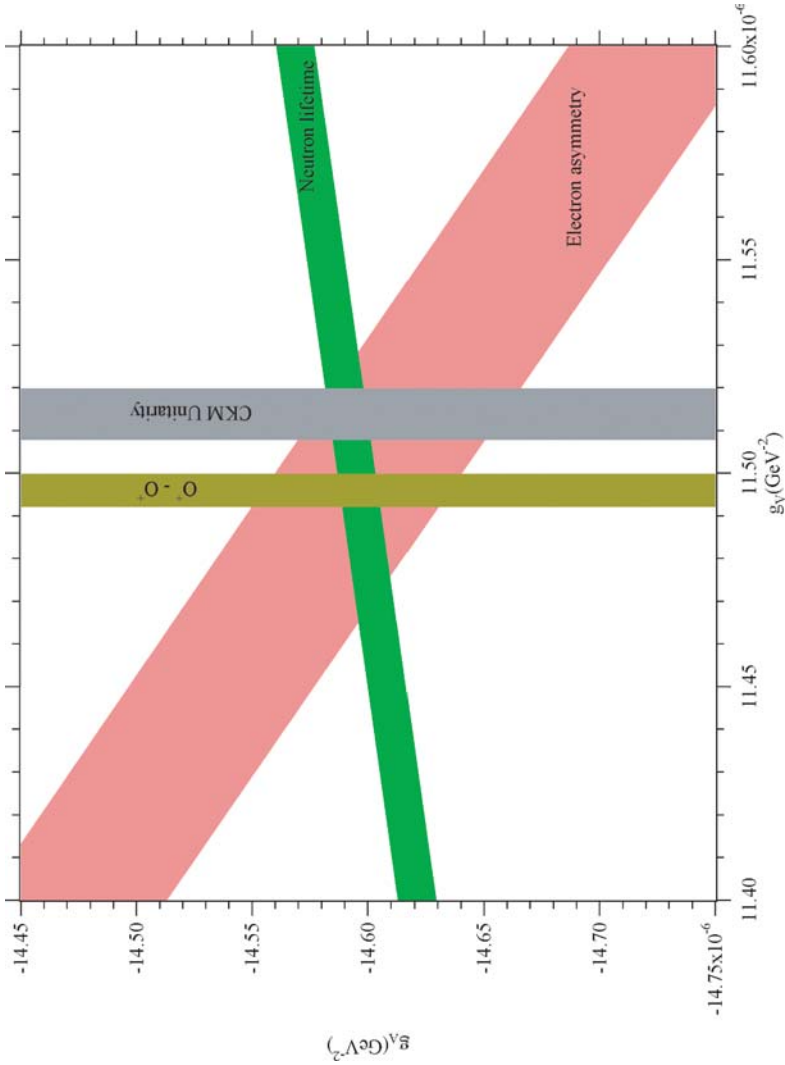


Figure 2 The weak coupling constants g_A and g_V determined from neutron decay parameters, $\mathcal{F}T$ values of superallowed $0^+ \rightarrow 0^+$ transitions, and CKM unitarity. For the neutron decay parameters, the width of the one-sigma band is dominated by experimental uncertainties. For the superallowed $0^+ \rightarrow 0^+$ transitions the uncertainty is dominated by radiative corrections.

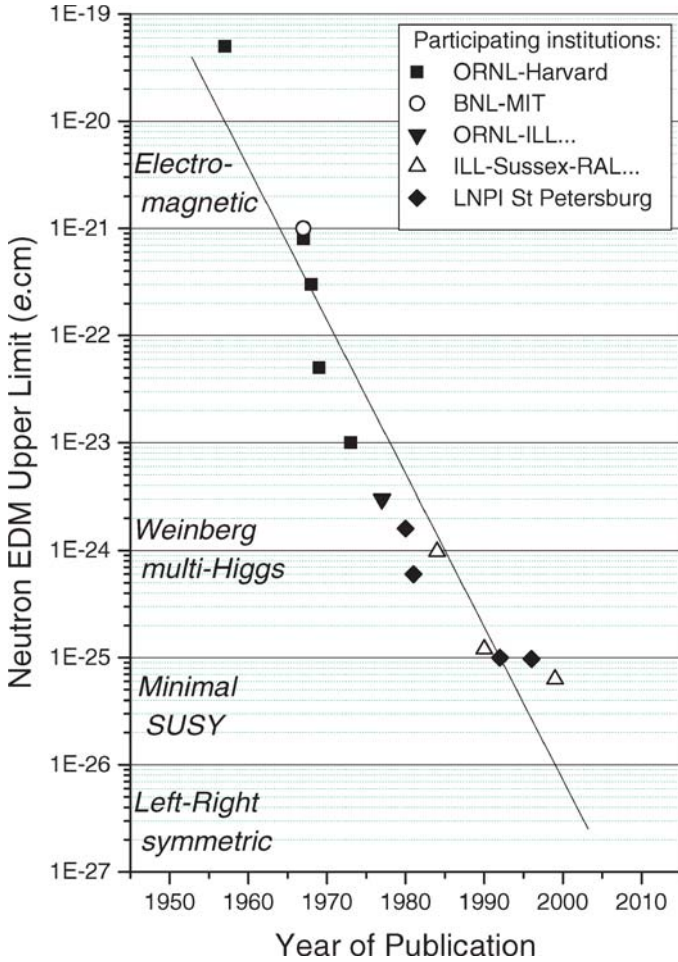


Figure 3 History of the neutron electric dipole moment limit and some of the ranges for different theoretical predictions. (Plot courtesy of P. Harris, University of Sussex.)

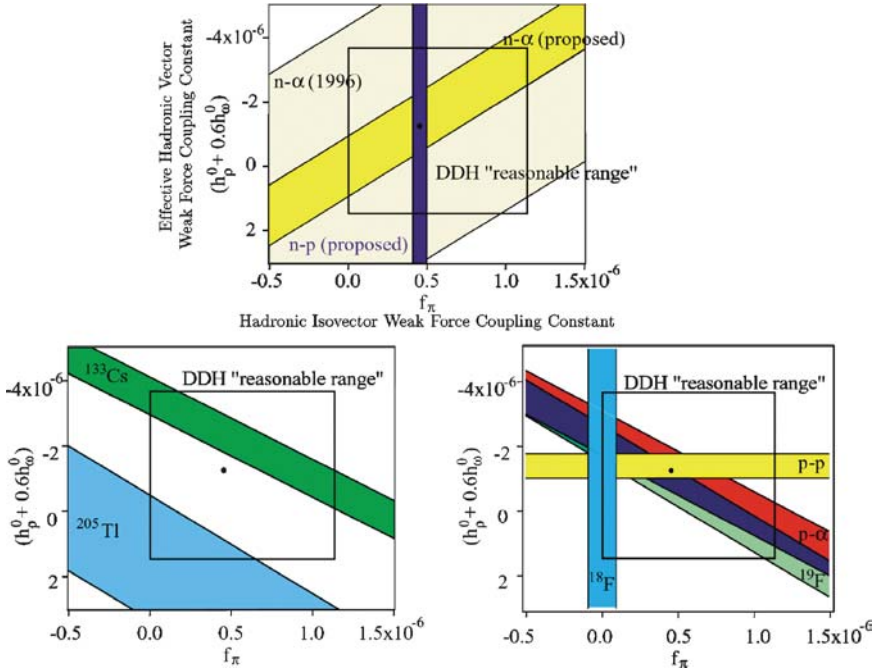


Figure 4 Constraints on linear combinations of isoscalar and isovector nucleon-nucleon weak meson couplings (178). The bottom graphs show constraints from measurements of anapole moments in ^{133}Cs and ^{205}Tl and from measurements in p - p and p - ^4He scattering and from ^{18}F and ^{19}F gamma decay. The top graph shows the anticipated constraints from proposed measurements of the P -odd asymmetry $p(\vec{n}, \gamma)d$ to 5×10^{-9} accuracy and the P -odd neutron spin rotation in ^4He to 2×10^{-7} rad/m accuracy. In each plot, the box indicates the reasonable range obtained by Desplanques et al. for the couplings.

CONTENTS

FRONTISPIECE, <i>D.H. Perkins</i>	xii
FROM PIONS TO PROTON DECAY: TALES OF THE UNEXPECTED, <i>D.H. Perkins</i>	1
FUNDAMENTAL NEUTRON PHYSICS, <i>Jeffrey S. Nico</i> <i>and W. Michael Snow</i>	27
TOWARD REALISTIC INTERSECTING D-BRANE MODELS, <i>Ralph Blumenhagen, Mirjam Cvetič, Paul Langacker,</i> <i>and Gary Shiu</i>	71
BLIND ANALYSIS IN NUCLEAR AND PARTICLE PHYSICS, <i>Joshua R. Klein and Aaron Roodman</i>	141
STUDY OF THE FUNDAMENTAL STRUCTURE OF MATTER WITH AN ELECTRON-ION COLLIDER, <i>Abhay Deshpande, Richard Milner,</i> <i>Raju Venugopalan, and Werner Vogelsang</i>	165
LITTLE HIGGS THEORIES, <i>Martin Schmaltz and David Tucker-Smith</i>	229
PHYSICS OF ULTRA-PERIPHERAL NUCLEAR COLLISIONS, <i>Carlos A. Bertulani, Spencer R. Klein, and Joakim Nystrand</i>	271
LEPTOGENESIS AS THE ORIGIN OF MATTER, <i>W. Buchmüller,</i> <i>R.D. Peccei, and T. Yanagida</i>	311
FEMTOSCOPY IN RELATIVISTIC HEAVY ION COLLISIONS: TWO DECADES OF PROGRESS, <i>Michael Annan Lisa, Scott Pratt,</i> <i>Ron Soltz, and Urs Wiedemann</i>	357
SMALL-X PHYSICS: FROM HERA TO LHC AND BEYOND, <i>Leonid Frankfurt, Mark Strikman, and Christian Weiss</i>	403
ASCERTAINING THE CORE COLLAPSE SUPERNOVA MECHANISM: THE STATE OF THE ART AND THE ROAD AHEAD, <i>Anthony Mezzacappa</i>	467
DIRECT PHOTON PRODUCTION IN RELATIVISTIC HEAVY-ION COLLISIONS, <i>Paul Stankus</i>	517
TOOLS FOR THE SIMULATION OF HARD HADRONIC COLLISIONS, <i>Michelangelo L. Mangano and Timothy J. Stelzer</i>	555